




Non-enzymatic electrochemical sensors for point-of-care testing: Current status, challenges, and future prospects

Christoph Bruckschlegel^a, Vivien Fleischmann^a, Nenad Gajovic-Eichelmann^b,
Nongnoot Wongkaew^{a,*} 

^a Institute of Analytical Chemistry, Chemo- and Biosensors, University of Regensburg, Universitaetsstrasse 31, 93053, Regensburg, Germany

^b Fraunhofer Institute for Cell Therapy and Immunology, Branch Bioanalytics and Bioprocesses, Am Muehlenberg 13, 14476, Potsdam, Germany

ARTICLE INFO

Handling Editor: Prof Agata Michalska

Keywords:

Non-enzymatic detection
Electrochemical sensors
Nanomaterials
Point-of-care detection
Wearable devices
Onsite detection

ABSTRACT

Current electrochemical sensors in point-of-care (POC) testing devices rely mainly on enzyme-based sensors owing to superior sensitivity and selectivity. Nevertheless, the poor stability, high reagent cost, complex fabrication methods and requirement of specific operational conditions make their adaptability in real-world applications unfavorable. Non-enzymatic electrochemical sensors are thus developed as they are more robust and cost-effective strategies. The advancement in material science and nanotechnology enables the development of novel non-enzymatic electrodes with favorable analytical performance. However, the developments are yet far from being adopted as viable products. This review therefore aims to gain insight into the field and evaluate the current progress and challenges to eventually propose future research directions. Here, fabrication strategies based on traditional and emerging technology are discussed in the light of analytical performance and cost-effectiveness. Moreover, the discussion is given on the pros and cons of non-enzymatic sensors when they are employed with various kinds of sample matrices, i.e., clinical and non-clinical samples, which must be taken into consideration for sensor development. Furthermore, molecular imprinting technology in tackling the selectivity issue is introduced and current progress is provided. Finally, the promising strategies from literature for solving the remaining challenges are included which could facilitate further development of robust POC testing devices based on non-enzymatic sensors. We believe that once researchers and technology developers have reached the point where most problems are solved, the non-enzymatic sensors are going to be the robust choice for POC testing in clinical diagnostic, ensuring food safety, monitoring contaminants in environment, and bioprocess control.

1. Introduction

In 2004, Wild et al. estimated that global diabetes cases would rise from 171 million in the year 2000 to 366 million by 2030 [1]. However, by 2021, diabetes already far exceeded this estimation, i.e., with 537 million people suffering from diabetes [2], a majority of whom resided in low- and middle-income countries. This significant deviation from projections not only raises questions about the current prevalence of diabetes but also highlights the urgency of developing affordable point-of-care (POC) sensors. This need is particularly critical in economically disadvantaged regions where access to advanced health-care facilities is rather limited. Such POC sensors will greatly enable individuals who are suffering from diabetes to monitor their blood

glucose levels inexpensively and without the need for elaborate laboratory tests.

POC sensors play a crucial role not only in diabetes management but also in addressing other diseases. The POC diagnostics market reached a substantial size of over 44 billion dollars in 2023, and it is projected to grow annually at a rate of 6.1 % until 2030. This remarkable growth is primarily driven by the increasing lifespan of people and the anticipated surge in cancer screening POC devices [3]. In addition, the recent pandemic has remarkably emphasized the necessity of POC testing that should be able to get access by anyone to allow disease containment in a rapid and effective manner.

POC sensors are mostly well known as clinical diagnostic tools where the test can be conducted at the site of or near the patient rather than in a

This article is part of a special issue entitled: Electroanalysis published in Talanta.

* Corresponding author.

E-mail address: nongnoot.wongkaew@ur.de (N. Wongkaew).

<https://doi.org/10.1016/j.talanta.2025.127850>

Received 29 November 2024; Received in revised form 30 January 2025; Accepted 26 February 2025

Available online 27 February 2025

0039-9140/© 2025 The Authors. Published by Elsevier B.V. This is an open access article under the CC BY-NC license (<http://creativecommons.org/licenses/by-nc/4.0/>).

laboratory, enabling medical intervention in a timely manner. Nevertheless, the beneficial features of POC devices, e.g., portability, providing rapid results, ease of access, user-friendly, and low cost, make them attractive in broader application contexts [4]. For example, in environmental monitoring they can be used for detecting contaminants in water, e.g., heavy metal and pesticide, facilitating prompt management and control of the harmful substances. Moreover, the on-site testing capabilities of POC sensors are highly beneficial for food and beverage industries in maintaining quality and safety of the products during production and prior to reaching the consumers, respectively. Furthermore, POC sensors are attractive for bioprocess industry where online monitoring of substrate consumption and product generation greatly facilitates the efficient process control and eventually provides high consistency and quality of desired products.

Electrochemical sensors are emerging as ideal candidates for POC applications due to their miniaturized design, rapid response times, robustness, cost-effectiveness, sensitivity, versatility, scalability, ease of use, low power consumption, and portability. Typical measurement methods used in electrochemical sensors include 1) amperometry, e.g., cyclic voltammetry, differential pulse voltammetry, or square-wave voltammetry, 2) potentiometry, and 3) impedance spectroscopy. Generally, the analyte can be detected either directly through oxidation or reduction of electroactive analytes, or indirectly, via affinity elements, e.g., antibody, and aptamer, that specifically bind to the analyte. The interaction in the latter case leads to changes in the current which can be monitored directly or indirectly through an additional redox marker.

Presently, commercially successful diagnostic tools in this domain are predominantly enabled by biosensors, with a strong reliance on enzyme-based systems [5]. This is not surprising as enzymes offer a superior combination of high selectivity, sensitivity, biocompatibility, and the ability to function effectively under physiological conditions. In principle, there are three generations of enzymatic biosensors that have been developed so far [6]. First-generation sensors rely on the measurement of current resulted from co-substrate (e.g., oxygen) consumption or co-product generation (e.g., H_2O_2) as a consequence of enzymatic reaction. However, electroactive interferences and the requirement of a sufficient amount of free oxygen in the samples make the first-generation sensors problematic. This issue has thus led to the development of the second-generation sensors which use synthetic mediators, e.g., ferrocene or osmium, for shuttling electrons between the enzyme's redox active center and electrode. Nevertheless, maintaining the presence of the redox mediator constantly near the electrode has proved to be challenging. As a result, the third-generation enzymatic sensors have been developed and aimed for promoting direct electron transfer between the enzyme and the electrode, eliminating the need for redox mediators. In this context, advances in nanostructures and porous materials have contributed to achieving mediator-free oxidation and reducing interference effects.

Although enzyme-based biosensors with various configurations have served as a goal standard platform for POC testing devices, they yet suffered from high material and fabrication cost [7–9], instability during sterilization, vulnerability to changes in temperature, pH or other environmental factors [10], the need for specific storage conditions, and short-term stability, that seek for more robust approaches. To overcome the challenges, there has been attempts to promote the detection of analyte of interest directly on electrode material which is considered as 'the fourth-generation sensor'. The term, e.g., 'non-enzymatic', 'enzyme-free', or 'enzymeless' has been used interchangeably for this type of sensors. In fact, analytes can be directly undergone redox reaction at any electrode. Nevertheless, electron transfer kinetics of many electrodes are too sluggish, thus requiring high overpotential to drive the redox reaction of interest. For example, a bare glassy carbon electrode (GCE) allows oxidation of glucose possible at 1.0 V–1.4 V (in an alkaline solution) [11]. Such high overpotentials are not favorable as they tend to cause side reactions, e.g., oxygen evolution, concomitantly occur with

the intended reaction, making the measurements of analyte at low concentrations troublesome. In addition, other electroactive species, e.g., ascorbic acid (AA), can easily undergo redox reactions at lower potentials, further generating false-positive signals. Therefore, researchers are attempting to develop electrodes that permit the redox reaction at relatively low over potentials.

Although the commercially available electrochemical sensors, e.g., glucose meter and FreeStyle Libre continuous glucose monitoring technology, rely mainly on enzyme-based detection strategy, the development of enzyme-free sensors plays a significant role in tackling the shortcomings of enzyme-based sensors. Here, apart from less expensive and more robust materials, the fabrication of enzyme-free sensors is generally much less complex than the immobilization of enzymes on electrodes, enabling more efficient control in the production process. Moreover, when electrodes require sterilization such as in case of FreeStyle Libre continuous glucose monitoring sensor, the whole production line of enzyme-free sensors does not need to be sterilized. The robustness of electrocatalytic materials makes the sterilization process possible after manufacturing. Overall, cheaper prices and greater reproducibility can be expected from enzyme-free sensors in comparison to the commercially available products. Furthermore, the longevity during storage of the enzyme-free sensors is possibly greater than the enzyme-based sensors as their functionality is less affected by the high temperature and humidity. This feature greatly facilitates the utility of the device in any country or areas where temperature and humidity during storage are deviated from optimal conditions. Additionally, less frequent calibration requirements could be expected from enzyme-free sensors as they are less prone to be affected from variability due to enzyme degradation. These beneficial features are likely the main driving force for more research and development to be conducted to push the enzyme-free sensors to commercial products, which have not yet been available so far.

Various kinds of electrodes have been introduced in which the significant progress in this field has been promoted majorly through the remarkable advancement in synthesis and fabrication of nanomaterials and nanostructures [12–14]. The research on enzyme-free sensors has been continually active over the past decade as can be seen from an

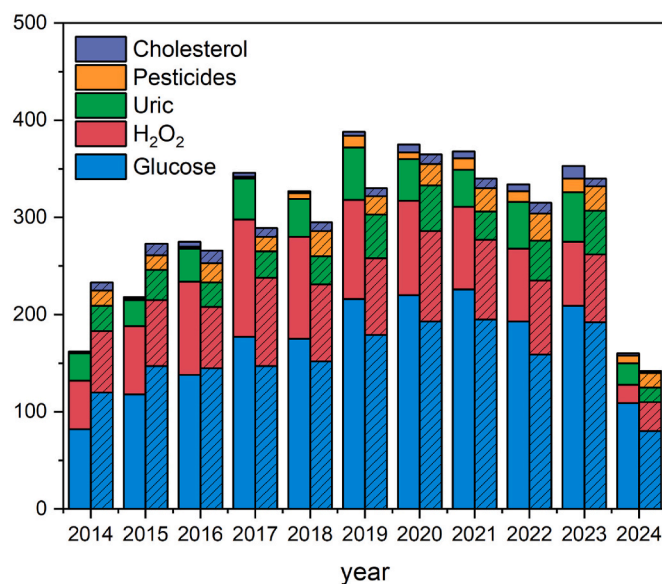


Fig. 1. The growth of research published in the past 11 years when searching with the terms "non-enzymatic electrochemical sensors", "enzyme-free electrochemical sensors", and "enzymeless electrochemical sensors" combined with the specific analyte (blank columns), and representation of the search with the same keywords but with enzyme-based strategies instead (patterned columns). Web of Science searched on July 2nd, 2024.

impressive high number of publications reported each year (Fig. 1). The numbers of enzyme-free sensors are considered highly comparable to the enzyme-based electrochemical sensors (Fig. 1: blank vs patterned columns). It is interesting to see that in 2016 enzyme-free sensors started to gain more attention when compared to enzyme-based strategies. Glucose, H_2O_2 , and uric acid have been widely investigated for both enzyme- and enzymeless sensors but pesticides and cholesterol have seen to rely majorly on using enzymes which suggests further research on enzymeless for these analytes.

Up to now enzyme-free sensors have been seen as a promising platform to address the needs for POC testing. However, most researchers attempted to develop novel electrode materials and improve analytical performance which have been successfully demonstrated mostly in ideal environments, e.g., pure buffer medium, where the electrodes can yield the greatest performance. Besides, the as-reported excellent sensing performance must be typically traded off with high costs of nano-material and fabrication methods, difficulty in large-scale manufacturing, and, for some cases, requirements of strict operational conditions, e.g., in alkaline media. Moreover, the biocompatibility of nanomaterials used for enzyme-free electrodes has been doubtful so far. These raise some crucial questions, i.e., are enzyme-free sensors able to be implemented in the field of POC testing, are there any restrictions/issues in using them, and what else should researchers do to facilitate the efficient translation of enzyme-free sensors into commercial products and to be practical in real-world applications?

In this review, we aim to provide a comprehensive overview of the entire development process for non-enzymatic electrochemical sensors (Fig. 2). First, we give the basic principles and mechanism of enzyme-free sensors to not only help non-experienced readers in entering the field but also define the scope of our review. This section also includes the discussion on the most common materials used in sensor development. We will then highlight the current state-of-the-art of fabrication methods for non-enzymatic electrochemical sensors and evaluate their advantages and disadvantages, particularly in the context of their implementation in POC testing devices. With this, we will highlight laser-induced non-enzymatic electrochemical sensors as an emerging technology that offers mass-production capability and high-performing electrodes at low cost. Additionally, we will critically evaluate specific sensor requirements for POC detection with respect to properties of sample matrices and the design of measurement and devices. This is crucial for researchers to consider from the onset in employing enzymeless sensor strategies in the development process based on the intended applications. Furthermore, as molecular imprinting technology has become a promising strategy to overcome selectivity issues, we thus will demonstrate advancements in this field and evaluate the possibilities and associated challenges when applied to enzyme-free POC testing. Finally, we will emphasize the remaining challenges and promising

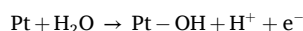
strategies that may apply in the future before giving conclusion and future prospects.

2. Definition, principle, and mechanism

To our knowledge, the term “non-enzymatic electrochemical sensors” or the other as-mentioned earlier have been ambiguously used for various meanings where it tends to broadly cover any electrochemical sensors without the use of enzyme. Therefore, it is not surprising to see the use of this term in many affinity biosensors, e.g., using molecular imprinted polymers, aptamers, or antibodies, and detecting changes upon analyte binding through impedance or signal blocking. However, in this review we will focus specifically on non-enzymatic sensors-based electrocatalytic reactions induced majorly by inorganic catalysts. In general, this type of non-enzymatic electrochemical sensors consists of a functional material embedded or modified on the electrode surface and an electrochemical signal can be obtained by catalytic reaction of the analyte [15,16]. Hereby, the functional electrode material enhances electron transfer kinetics, i.e., lowering the required potential compared to pristine electrodes [17]. Various kinds of functional material have been reported for this purpose, namely 1) metal- or metal oxide-based materials, e.g., noble and transition metal and their composites, 2) carbon-based materials, e.g., graphene and its derivatives, and 3) combinations of carbon and metals or metal oxide.

In non-enzymatic detection, electrocatalysts play an important role in triggering redox reaction of the analyte. To understand the basic mechanism, an exemplary catalytic reaction of glucose, the most-studied analyte, is discussed as follows. Catalysis is in fact a complex topic, and in principle, each catalyst material could follow a different mechanism. Additionally, for a single catalyst, multiple adsorption geometries can exist [18], and even the crystal plane facing the analyte significantly influences the catalytic properties [19]. However, by simplifying this topic and reducing it to a common denominator, we can generally distinguish between two fundamental mechanisms, i.e., 1) reactions-based on noble metal surfaces and 2) reactions-based on non-noble metal surfaces.

Both mechanisms basically involve hydroxide species adsorbed on the surface. However, noble metal can possibly catalyze its reaction in neutral conditions, while base metal usually requires basic conditions. For noble metals, e.g., Pt or Au, at neutral pH, water can be oxidized at low potentials on their surface, forming a covalently attached layer of hydroxide species according to the ‘Incipient Hydrous Oxide Mediator (IHOM)’ model:



According to the concentric adsorption theory, glucose also adsorbs on the surface of the noble metal by breaking the bond between the

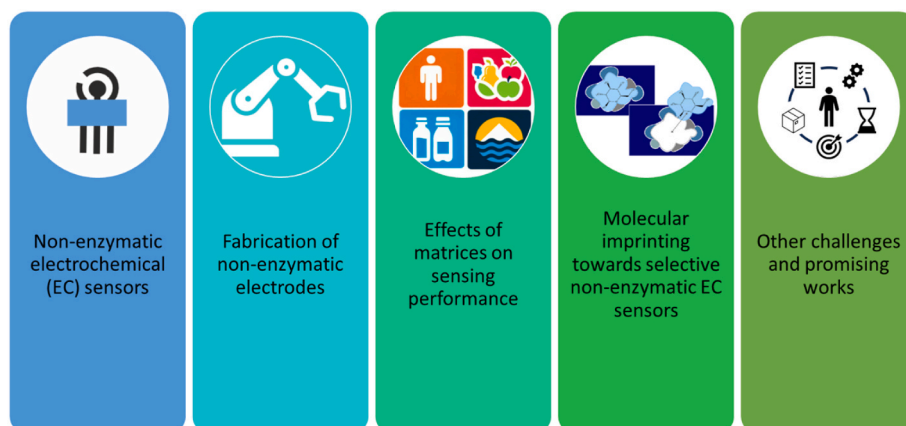
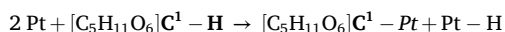


Fig. 2. Structure of this review.

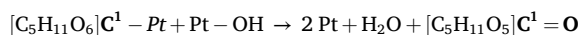
hydrogen atom and the C₁-atom of glucose



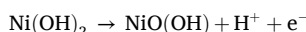
The hydrogen-atom is then oxidized:



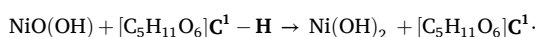
Both the covalently bound hydroxide species and the glucose subsequently react with each other on the Pt surface to form gluconolactone and water:



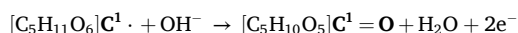
In contrast, for non-noble metals such as Ni or Cu, basic conditions are required to form hydroxides such as Ni(OH)₂. These hydroxide ions are not covalently bound but interact ionically instead. During oxidation of Ni(OH)₂ in a basic medium, Ni(III) oxyhydroxide is formed



This species can abstract the hydrogen atom at the C¹ atom in glucose in a rate-determining step, forming radicals:



The radical further reacts with a hydroxide ion to form gluconolactone and water:



In summary, on the catalyst surface of noble metals, water is first oxidized, and hydroxide is covalently bound to the noble metal. Additionally, glucose can adsorb to the surface by breaking the bond between the C1 and hydrogen atoms, with both fragments being covalently bound. The glucose fragment then reacts with hydroxide to form gluconolactone. In contrast, for non-noble metals, hydroxide ions must be present in solution (basic conditions), and glucose is oxidized by the strong oxidant generated, i.e., Ni(III) oxyhydroxide. Considering both mechanisms, the key difference between noble and base metals lies in their electron composition. Here, the 5d orbitals of Pt (electron configuration: [Xe]4f145d96s1) or noble metals in general, effectively overlap with the orbitals of glucose due to their geometric size and energy levels. This overlap enables the adsorption of glucose and direct participation in redox reactions [20]. On the contrary, non-noble metals such as Ni (electron configuration: [Ar]3d84s2) only have 3d orbitals, which are likely unable to interact with other molecular orbitals as effective as 5d orbitals. Therefore, the surrounding hydroxide species are necessary to enable electrocatalytic oxidation of glucose.

Here, Table 1 gives a summary of the most common metal nanocatalysts for glucose as an example analyte.

The recent review article by Nemati et al. showed a comparison of analytical performance between enzyme-based and enzyme-free sensors for glucose [29]. The comparison of sensitivity per electrode's area has shown that enzyme-free sensors yielded two to four orders of magnitude greater than that of enzyme-based sensors. This may be attributed to the unhindered accessibility of analytes towards the electrocatalytic surface. As a result, the enzyme-free sensors generally tended to offer lower detection limits in comparison to the enzyme-based sensors. Nevertheless, it is worth noting that enzyme-based sensors could be slightly more sensitive than enzyme-free sensors as reported by Lee et al. [30]. This superior feature has to be, however, traded off with tedious steps involved in enzyme immobilization that promote the exposure of functional enzyme active sites with proper orientation.

3. Fabrication of non-enzymatic electrodes

3.1. Conventional strategy

3.1.1. Drop-casting and dip-coating

Drop-casting and dip coating are straightforward methods used to

Table 1

Most common metal nanocatalysts used for enzyme-free glucose sensors.

Category	Example	pros	cons
Nobel metal	Pt [21], Au [22]	- good stability - operation under physiological pH	- expensive - surface poisoning issue
Non-nobel metal	Ni [23], CuO [24], Co ₃ O ₄ [25]	- inexpensive - less prone to surface poisoning and electroactive interfering species	- requirement of basic condition
Multimetal (bi- or trimetallic alloy)	Pt/Au [26], Pt/Ni [27], Au/Ni [28]	- Enhancement of current response - Improving the catalyst's resistance to interference - Reducing cost when combined with non-nobel metal - Feasibility for multiple analyte detection - Facilitating <i>in situ</i> OH ⁻ generation by nobel metal, e.g., Au, thus enabling catalytic reaction by the adjacent non-nobel catalyst, e.g., Ni.	- complexity in synthesis to achieve favorable electrocatalytic properties

modify the surface of an electrode with nanocatalysts. In drop-casting, catalyst material suspension in a small volume is placed and adsorbed directly onto the electrode, while in dip coating, the electrode is normally immersed in the catalyst solution which requires a greater volume of suspension. The former technique is superior in terms of material usage, as the catalyst material is selectively deposited only on the electrode's surface, unlike the latter one. After electrode drying, the modification process is complete. Although both methods are highly facile and widely employed for generating enzyme-free POC sensors, the major drawback of these methods is the inhomogeneous distribution of the catalyst material caused by the coffee ring effect occurred during liquid evaporation [31]. Here, as liquid evaporates from the edge, it is replaced by interior liquid, thus creating radial flow. This flow carries dispersed material to the edge, resulting in a characteristic ring pattern. To mitigate this effect, co-solvents with low evaporation rates and higher viscosity can be added [32,33]. These two properties will reduce the driving force of radial flow and increase resistance towards radial flow, respectively. Furthermore, various other attempts have been conducted to overcome the issue as reviewed by Kumar et al. [31]. These include (i) using substrates with super hydrophobic surfaces [34], (ii) employing electrowetting [35], (iii) utilizing anisotropic particles [36], (iv) introducing surface acoustic waves [37], and (v) enhancing Marangoni flow [38]. Among these, adjusting the solvent to enhance the Marangoni flow (e.g., using a mixture of solvents with different surface tensions) and using anisotropic particles appear to be the most practical solutions.

3.1.2. Electro- or electroless deposition

Electro- or electroless deposition is a technique that has gained prominence in the field of enzyme-free sensors. In case of electrodeposition, ion precursors from the surrounding solution deposit on the electrode by applying an oxidative or reductive potential. Alternatively, the formation of metal ion precursors into catalyst nanoparticles is also feasible without application of external potential, termed electroless deposition. For example, Kawakami et al. electropolymerized polypyrrole onto Pt electrode followed by drop-casting KAuCl₄ solution on the as-prepared electrode [39]. After drying, AuNPs with diameters ranging from 20 to 40 nm, depending on the volume of KAuCl₄ solution

introduced, were formed and the electrodes were used for glucose detection. Both methods are a highly controllable manner with relatively high precision. Here, the morphological structures and sizes of nanocatalysts obtained from electrodeposition can be precisely controlled by fine-tuning the solution compositions, time, and/or the applied current and potential [40]. Similarly, the nanocatalyst features based electroless deposition can be controlled via chemical compositions introduced, deposition time, and/or volume used for deposition [39]. In addition, the techniques allow ones to exclusively deposit the nanoparticle catalysts on the specified working area, thus avoiding contamination to any other unwanted sensor components.

Nevertheless, during electrocatalytic reaction the deposited nanocatalyst films can be unstable and peeled off from electrode surface easily. To address the issue, Viswanathan et al. used methionine to strengthen electrodeposited copper-cobalt nanostructures on indium tin oxide (ITO) electrodes [41]. Hereby, the thiol group of methionine interacts with metal ions (Cu^{2+} and Co^{2+}) during electrodeposition. This interaction stabilizes the films by forming a protective layer on the electrode surface, preventing the detachment during electrocatalysis. Apart from instability during electrocatalysis, mechanical force such as from solution stirring can raise the issue during sensor operation, especially when deposition of nanocatalysts is carried out on 3D-porous electrodes containing high number of edges and defects. Our research group has demonstrated that under shaking at 50 rpm continuously for 5 h, nearly 100 % of the electrodeposited Ni nanoparticles on carbon nanofiber electrode detached from the surface [42]. The electrodeposition of nanocatalysts on 3D-porous carbon or any rough surface electrodes can suffer from poor adhesion stability apart from poor fabrication reproducibility. Therefore, leaching study is mandatory to carry out when sensor operation has to be performed inline, real-time, and under flow-condition.

3.1.3. Printing

3.1.3.1. Screen-printing. Screen printing, a versatile, cost-effective, and user-friendly technique, is commonly used for manufacturing electrochemical sensors [43]. It relies on applying conductive ink such as carbon and metallic inks, or their mixture onto a substrate support, e.g., ceramic or plastic, using a screen mesh containing electrode patterns [43]. The formulation of conductive ink is critical in this process. Typically, the inks consist of conductive material such as carbon or metal powder/particles to ensure electrical conductivity, and additional binders to enhance interactions between the conductive material and the substrate as well as the material itself [43]. Here, solvents regulate ink rheology and viscosity, and importantly aiding printability [43]. Additionally, some additives, e.g. surfactants or chelating agents, are introduced to improve wettability and drying rate, and prevent agglomeration of conductive particles [43]. However, the use of binders and other additives, while essential in ink formulation, can lead to poor electron transfer kinetics of the embedding nanocatalysts, necessitating surface activation prior their uses of electrodes [43]. The electrode surface can be activated by electrochemical pretreatment or plasma treatment to improve electron transfer kinetics. The study shown by Su et al. demonstrated the effect of electrochemical pretreatment procedures with varying scan ranges and observed significant changes such as increased porosity, enhanced electron transfer kinetics, and a larger effective surface area [44].

In principle, catalytic functionalities such as metal nanoparticles can be directly incorporated into the ink to fabricate enzyme-free sensors by screen printing. However, to our knowledge, there are relatively few publications on this method which is probably due to the challenge on preventing nanoparticle agglomeration within the ink [45,46]. Agglomeration, especially during drying, leads to the formation of larger particle clusters, diminishing the overall high catalyst surface area achieved by the nanometric size of the nanoparticles. Addition of

stabilizing agents to prevent agglomeration of nanoparticles is possible but their excess amount can adversely reduce viscosity and subsequently diminish printability [47]. Furthermore, since nanoparticles are distributed throughout the entire ink (not just on the surface), the portion of nanoparticles contributing to the catalytic reaction is significantly lower than the total number of nanoparticles added. This aspect is especially important when working with costly catalyst materials, e.g., platinum or gold nanoparticles.

For real-world applications, a screen-printed electrode that does not require pretreatments to overcome the limitations of additives would be highly beneficial. Therefore, the catalyst material in the binder-free ink must exhibit thixotropic properties to ensure printability. In their comprehensive review, Suresh et al. proposed that water-based ink containing rGO nanofibers could be particularly interesting [43]. The basic idea is that the catalyst material itself includes structural elements necessary to use as printable ink. We suggest that these rGO nanofibers could be functionalized, for example, by attaching nanocatalysts prior to performing ink formulation. To name an example that proofed such approaches, Abdolhosseinzadeh et al. used MXene sediments, which are two-dimensional inorganic compounds consisting of carbides and nitrides of transition metals, to formulate an additive-free ink with suitable rheological properties [48].

3.1.3.2. Inkjet printing. Inkjet printing is a versatile, fast, and low-cost production method for creating electrochemical sensors. Inkjet printing means that we can print an electrode directly on a substrate with a commercial inkjet printer. Its high adaptability stems from the fact that no masks are needed, unlike screen printing or photolithography [49]. Lab-compatible inkjet printers, such as the EPSON L130 [50], are affordable (available for under €300) and can be used with ink tanks instead of ink cartridges for easier refilling purposes. The printing process efficiently utilizes inks and is highly scalable [49]. Substrates for inkjet printing range from commercial A4 paper [50] to flexible polyethylene terephthalate (PET) plastic [49]. However, precise ink formulation is crucial. While screen printing can handle higher ink viscosities and solid loadings, inkjet printing may face nozzle clogging and printability issues [51]. Additionally, the wettability of the ink on the substrate impacts overall resolution, which can be fine-tuned through ink formulation or substrate treatment [51]. For inkjet printing, the coffee ring effect (cf. To 3.1.1) plays a crucial role, but can be solved by the same strategies as mentioned for drop-casting or dip coating method. In addition, nanofibers, e.g. cellulose nanofibers in aqueous solution, could effectively reduce the coffee-ring effect by preventing the rush hour phenomenon, which is a drastic acceleration of radial flow at the final stage of the drying [52]. However, a possible nozzle clogging needs to be kept in mind with these approaches.

There have been attempts to formulate the ink by combining nanocatalysts with carbon nanomaterials such as graphene [53,54]. However, metal nanoparticles without carbon matrix can be successfully fabricated via inkjet-printing method as well as demonstrated Ahmed et al. [55]. Hereby, the authors ensured homogeneity of the ink solution made of copper oxide nanoparticles by filtering through a 0.45 μm -membrane. However, to improve conductivity when electrodes are printed on substrates like paper, it may be necessary to print repeatedly on the same position [54]. Similar to screen-printing, additive free approaches using MXenes exist and have been successfully used for printing electrodes on textiles [56].

3.1.3.3. 3D-printing. Three-dimensional (3D) printing is a versatile and cost-effective technique to create electrochemical sensors [57]. One significant advantage of 3D printing is the ability to produce complete, customized analytical systems. In addition to using conductive filament for the electrode, non-conductive filament can be employed for support or surrounding structures. However, there are some drawbacks to 3D-printing approach. The specialized knowledge required for 3D

design software and the steps involved in transitioning from a 3D model to a physical print can be challenging. Additionally, the cost of 3D printers varies significantly, ranging from as low as US\$ 150 to as high as US\$ 8300, depending on specifications such as resolution, compatible polymers, and dual nozzle printer for a faster printing when more filaments are used [57]. Customized conductive filament contained additive nanocatalysts also requires a filament extruder. Despite these challenges, there are user-friendly 3D modeling software options available, such as Autodesk's Fusion 360. These programs allow users to export STL files after designing their 3D models. The next step involves using a "slicer" software (such as PrusaSlicer) that converts the STL file into a "G-code" file—a set of precise instructions for the 3D printer.

Commercial polylactic acid (PLA) conductive filament, e.g., Black Magic 3D Conductive Graphene Composite® (graphene contained PLA), can be used for printing 3D structure of electrode support. However, to construct non-enzymatic sensors, electrocatalysts have to be introduced via post-treatments such as electrodeposition. The technique is considered inconvenient, leading to many attempts in the direct incorporation of electrocatalysts into the filament to avoid such issue. For example, Rocha et al. synthesized $\text{Ni}(\text{OH})_2$ microparticles and mixed them with a commercial conductive filament, which was cut into small pieces, in a proper solvent prior to drying and subsequently extruding into a filament for 3D printing [58]. However, the 3D-printed electrode requires polishing and electrochemical activating steps before detecting glucose performed in alkaline conditions.

3.1.3.4. Roll-to-roll (R2R) printing. Compared to previous printing techniques, Roll-to-Roll (R2R) printing works like a stamp which is alternately immersed into an ink and pressed onto the substrate. With that, R2R is a fast and high-throughput technique with low adaptability for sensor design and a significant entry barrier due to the investment required for R2R printing machines. Additionally, drying chambers are typically needed after each printing step, consuming a substantial amount of energy. However, once the design is finalized and the printing parameters, as well as ink formulation (rheology, printability, surface tension, and stability), are optimized, the major advantage of R2R printing is its high throughput. Furthermore, additional electrodes containing different materials can be added consecutively by using additional printing rolls.

Substrates for R2R printing are typically thin polymer films such as PET [59–61] and flexible polyimide [62,63]. There are two promising R2R printing techniques: 1) R2R gravure printing and 2) flexography.

R2R gravure printing (Fig. 3-left) [59], a metal cylinder with a gravure (the negative imprint of the sensor design) dips into the ink solution. A doctor blade removes excess ink that is not in the engraved cavities of the roll. After the doctor blade, the ink-loaded gravure roll contacts the substrate, which is guided by the impression cylinder, transferring the ink to the substrate. As demonstrated by Bariya et al. multiple layers of various materials can be printed in a continuous process where the finished printing layer in each step is subjected to drying in between. The authors demonstrated that 150,000 electrodes on a 150 m-long PET substrate with multiple materials can be printed within only 30 min [59].

In flexography (Fig. 3-right) [63], ink is transferred onto the anilox roll, which has uniformly distributed engraved cavities capable of loading a defined amount of dye. After the removal of excess ink by a doctor blade, the defined amount of ink is transferred to the flexo plate which contains a positive imprint of the sensor design. The ink on the flexo plate is then transferred to the substrate on the impression cylinder. Fung et al. used flexographic printing on a polyimide substrate to consecutively print an Ag/AgCl reference electrode, a carbon working and counter electrode, and a zinc acetate precursor layer on top of the working electrode. After each step, the ink was dried at 150 °C for 10 min. During heating, the zinc acetate precursor formed zinc oxide (ZnO) nanowires. Even though the authors employed electrodes for enzymatic glucose sensors the strategy is highly practical for enzyme-free sensors.

Comparing both methods, R2R gravure printing offers exceptional detail and high volumes, but it comes with a high upfront cost due to the need for cylinder engraving, making it an ideal technique for high-volume prints. Furthermore, it is more limited in terms of absorbent substrate material. Flexography, on the other hand, has lower upfront costs and setup time due to the easier adaptability of the flexo plate and is suitable for various substrates, making it an ideal candidate for lower volumes and more individualized prints due to its easier adaptability.

3.2. Laser-induced functional hybrid electrodes as emerging technology

Laser-induced catalyst synthesis is a promising single-step preparation method for non-enzymatic electrodes, as both the embedded catalyst and the conductive material, i.e., laser-induced graphene (LIG) can be generated simultaneously, forming a functional hybrid material [17]. A wide range of precursors can be used for fabrication of LIG, including polymers such as polyimide, wood, cloth, or paper [17]. During the laser scribing process, the substrate is carbonized, resulting in a reduced

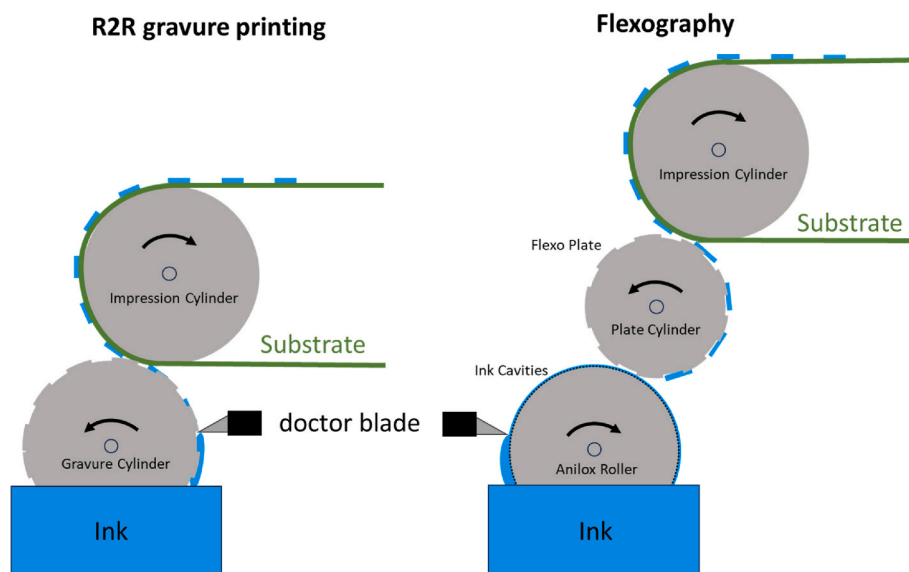


Fig. 3. Setup of Roll to Roll (R2R) printing (left) and Flexography (right).

graphene oxide-like structure. This method is fast, inexpensive, and easy to adapt as electrodes can be scribed in any pattern. Furthermore, it enables 3D-porous electrodes with immense surface area which is highly favorable for sensor development. The size, structure, and composition of LIG are highly dependent on the laser settings, e.g., power, speed, scribing mode, lens, atmosphere, and the laser power needed to convert material to LIG is very dependent on the thickness and composition of the precursor. In 2015, Tour's group conducted pioneering work by *in situ* generating metal oxide nanoparticles embedded within LIG using a CO₂ laser ($\lambda = 10.6 \mu\text{m}$) in which a metal salt-containing polyimide film was used as the precursor material [64]. The functional hybrids have been used for oxygen reduction reactions in the field of energy conversion and storage. This pioneered work has significantly enabled the fabrication of many novel carbon nanocatalyst hybrids for enzyme-free electrodes used in POC testing (Fig. 4). In this section, discussion will be given based on how the substrate precursor is prepared prior to laser exposure.

3.2.1. Coating catalyst precursor on carbonizable substrate

To introduce metal nanocatalysts, coating a polyimide film substrate with metal precursors has been demonstrated (Fig. 4A). For example, Fan et al. covered a polyimide film with a thin metal leaf, e.g., gold, silver, platinum, palladium, and copper, prior to laser scribing the material using a CO₂ laser [65]. In addition to generating monocatalyst-graphene hybrid, the authors also demonstrated that AuAg alloy could be facily obtained via the combination of gold and silver leaf coating. The AuAg alloy LIG electrodes were successfully employed as enzyme-free electrodes for glucose detection in blood plasma sample. Although the authors have shown superior analytical performance, the stability of the as-generated nanoparticles remains a question as the initial interaction between metal leaves and PI substrate could be very weak. The nanocatalysts might be weakly bound to the LIG surface after scribing which may raise stability issue when applying the electrodes under stirred- or flow-condition. Furthermore, applying very thin metal leaves may cause poor reproducibility when the process is not well-controlled. The method could be possibly circumvented through making a mixture of metal precursor together with a polymer matrix and homogeneously coated on a polyimide substrate as recently proposed by Zhang et al. [66]. Here, the mixture of Cu²⁺ precursor and ethyl cellulose in ethanol was spin-coated on a polyimide substrate. The ethyl cellulose may assist the spinning process and/or adhesion stability between precursor and polyimide film substrate. After drying the polymer film, a copper-embedded graphene electrode was generated using a CO₂ laser. The authors successfully applied the resulting electrodes for determination of glucose in beverages. Similarly, Zhao et al. knife-coated a polyamic acid mixed with Co²⁺ precursor on a polyimide substrate film and laser-generated Co₃O₄ nanoparticles-graphene hybrids [67]. Here, polyamic acid is considered a carbon precursor and needs to be converted into polyimide via imidization process under high temperatures, e.g., 180 °C, prior exposure to the CO₂ laser. Unlike using ethyl cellulose as a matrix, the Co-doped PI layer could adhere better to polyimide layer underneath.

3.2.2. Blending catalyst precursor with carbonizable substrate

Although coating catalyst metal precursor on a carbonizable substrate, e.g., polyimide or Kapton, is high facile, direct doping the metal catalyst precursor with graphitizable materials (Fig. 4B) is considered more effective as homogeneous distribution of catalysts through the entire 3D-electrodes can be expected. In this regard, the polymer precursor can be prepared similarly to the work proposed by Tour's group where polyamic acid precursor is blended with metal salt and later converted into metal-doped polyimide prior to laser scribing without the need of polyimide film underneath [64]. Alternatively, a solvent soluble polyimide (Matrimid® 5218) is commercially available which allows direct preparation of metal salt-doped polyimide precursor without the need of imidization process. Our group has employed this material to

create electrospun carbon nanofibers doped with nanocatalysts for non-enzymatic electrochemical sensors. For example, in the pioneered work, the spinning solution made from nickel acetyl acetate blended with Matrimid® 5218 was electrospun and later subjected to CO₂ laser for generating Ni embedded laser-induced carbon nanofibers (Ni-LCNFs) [42]. The electrospun nanofibrous precursor facilitates the formation of 3D-porous structure and the homogenous distribution of Ni nanoparticles. The Ni-LCNF electrodes enabled glucose detection in sub-micromolar range which is attributed to high surface area and immense porosity of the electrodes. In addition, we have proven that the stability of Ni within LCNFs is higher than the electrodeposited Ni counter parts when the electrodes were subjected to stirring condition. We also later generated Pt-LCNF electrodes and successfully employed them for H₂O₂, highlighting the versatility of the strategy.

Apart from the polymers mentioned earlier, graphene oxide film mixed with metal precursor has been proposed. For example, recently, Scroccarello et al. prepared a film substrate by filtering a suspension of graphene oxide blended with metal salt, e.g., Au³⁺, Ag⁺, or Pt²⁺ [68]. After drying the film coated filter paper, non-enzymatic working electrodes were generated using CO₂ laser. The authors have demonstrated the utility of their electrodes, namely Au@rGO-, Ag@rGO-, and Pt@rGO for determination of caffeic acid, nitrite, and hydrogen peroxide, respectively, with detection limits in sub-micromolar range. Nevertheless, the sensor manufacturing still requires transferring the metal/rGO film onto an additional substrate where counter and reference electrodes were accommodated. This may subsequently lead to poor reproducibility of the sensors due to additional steps required.

Both coating and blending strategies are highly promising for upscaling the manufacturing process of non-enzymatic sensors. In comparison to the screen-printing technique, the 3D-porous structure of laser-generated non-enzymatic electrodes allows more efficient contact between analytes and catalysts anchored or embedded within LIG. However, to reach this favorable characteristic, wettability of LIG electrodes must be ensured as the roughness and microstructures could make the electrode surface highly hydrophobic, hindering the access and contact to the inner porous structure. Plasma or UV-zone treatment, and introduction of surfactant in the measuring samples could be conducted to hydrophilize LIG-doped nanocatalyst electrodes. Nevertheless, it is also necessary to ensure that such treatments do not adversely affect to the capability of nanocatalyst.

Table 2 summarizes the fabrication techniques discussed in this chapter.

4. Effects of matrices on sensing performance

4.1. Clinical sample

4.1.1. Blood

Blood is undoubtedly the most accurate biofluid in terms of analyte concentration found in the body and widely used sample in clinical settings and POC testing as seen from glucometers commonly used by diabetic patients. As analytes in blood are typically present in high concentrations (e.g., glucose levels ranging from 3.9 to 5.6 mmol/L) [69], the detection does not need highly sensitive enzyme-free electrodes. Instead, the sensor development should rather focus on selectivity and antibiofouling strategies due to the numerous interfering substances present. Since catalytic reactions are usually pH-dependent, all measurements and optimizations should be ideally carried out at the blood pH, i.e., 7.3–7.4 [70], in order to enable a direct measurement without the need for sample preparation steps like pH-adjustments.

In selectivity studies, it is essential to consider key substances that can be easily oxidized or reduced during electrochemical measurements, depending on the potential used for analyte detection. Notably, urea and lactate are significant molecules commonly found in blood, with average concentrations around 5 mmol/L (tending to increase with age) [71] and below 2.2 mmol/L [72], respectively. In enzyme-free sensors, the

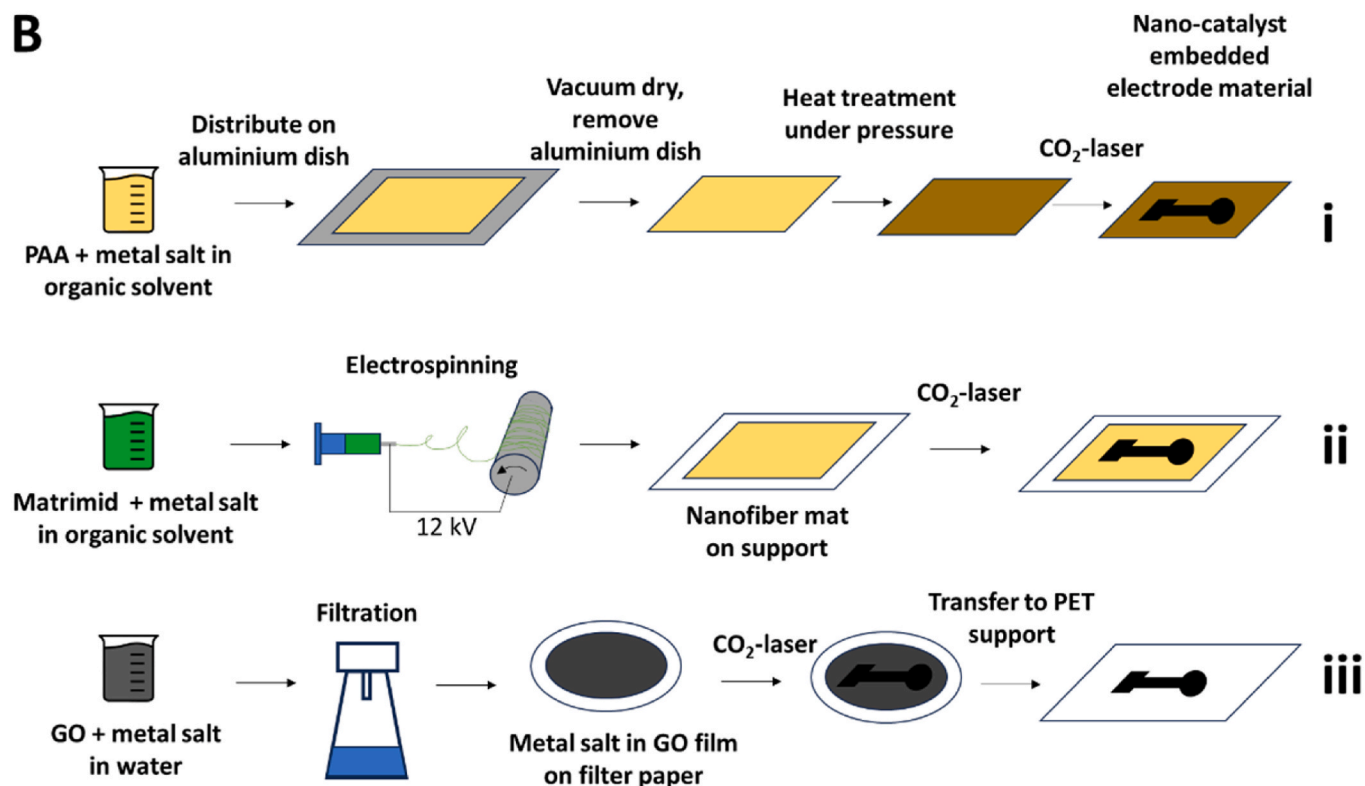
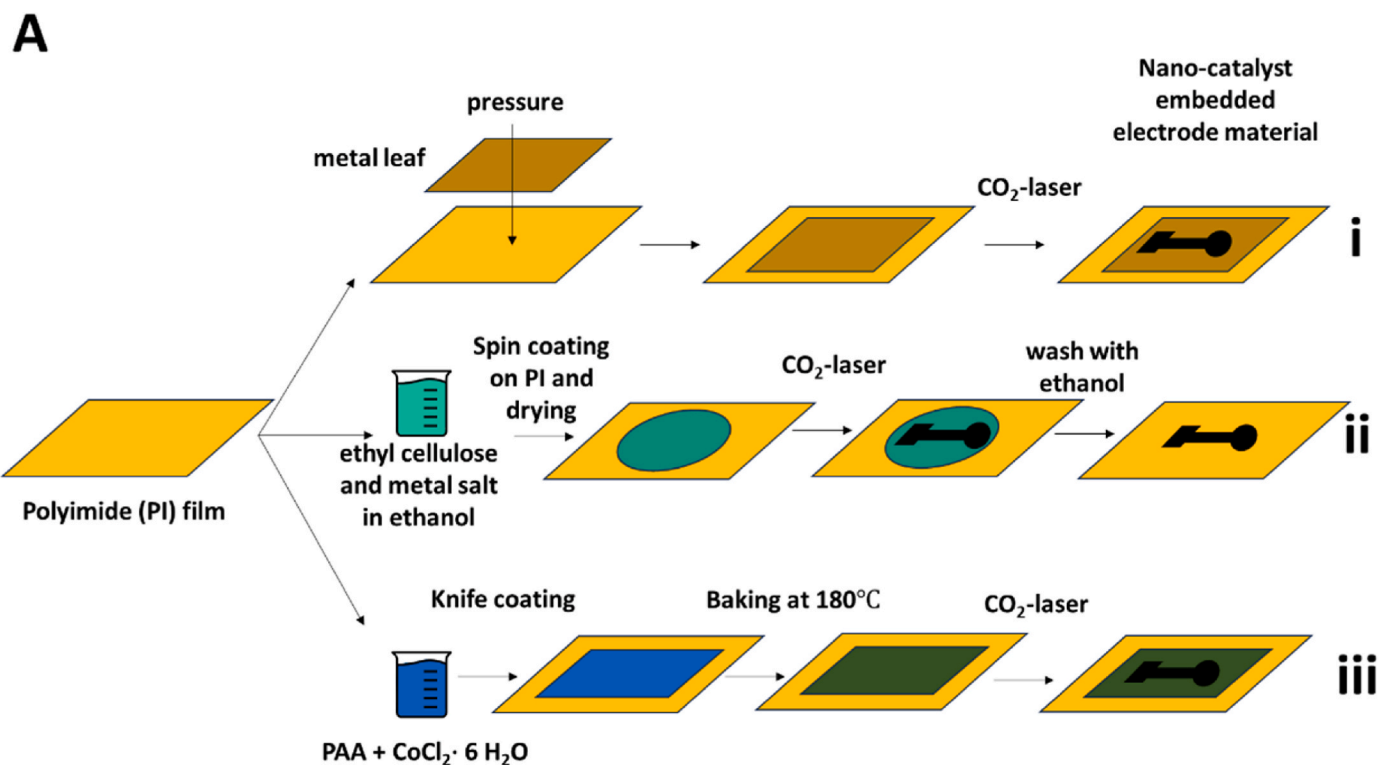


Fig. 4. Fabrication of enzyme-free electrodes using CO₂ laser. (A) Coating catalyst precursor on carbonizable substrate: (i) attaching a metal leave on polyimide (PI) substrate, (ii) spin coating a PI substrate with an ethyl cellulose + metal salt solution, and (iii) by knife coating a PAA + metal salt solution onto a PI substrate. (B) Blending catalyst precursor with carbonizable substrate: (i) distributing polymer-metal salt solution on a surface, drying, and a consecutive heat treatment, (ii) electrospinning a polymer-metal salt solution, and (iii) by preparing a graphene oxide (GO)-metal salt solution and consecutive filtration. The schemes were drawn as described in Refs. [42,64–68].

Table 2
Comparison of fabrication techniques.

Strategy		Complexity and cost of instrumentation	Fabrication throughput/mass production capability	Strengths	Weakness
Conventional method	Drop casting & dip coating	Low	High	Simple, cheap	Coffee-ring effect, stability (leaching), base electrode needed
	Electro- or electroless deposition	Low - Moderate	Low - Moderate	Simple, cheap, selective (coating only on working electrode)	Electrodeposition on each individual electrode, stability (leaching), based electrode needed
	Screen printing	Low - Moderate	Moderate - High	Simple, cheap, complete electrode is produced, few manufacturing steps	Need of a mask, surface activation needed, support needed
	3D printing	High	Low	Very complex and individual systems printable, complete electrode is produced	Slow, expensive, surface activation needed
	Roll-to-roll printing	High	High	Very high throughput, perfect for upscaling, complete electrode is produced	Very expensive machine, offset print (hard to customize), support needed
Laser-induced functional hybrid as emerging technology	Coating catalyst precursor on carbonizable substrate	Moderate	Moderate - High	Simple, cheap, complete electrode is produced, few manufacturing steps	Carbonizable substrate needed, laser scribe is expensive
	Blending catalyst precursor with carbonizable substrate	Moderate	Moderate - High	Simple, cheap, complete electrode is produced, freestanding material is possible, few manufacturing steps	Laser scribe is expensive

same catalytic strategy, e.g., nickel oxide species in alkaline conditions, not only allows oxidation at similar potentials for both urea [73] and lactate [74] but also glucose [42]. Therefore, careful attention has to be paid to the selectivity when one of these analytes is measured by non-enzymatic approach. Additionally, antioxidants like uric acid or ascorbic acid, both present in blood with concentrations at around 500 $\mu\text{mol/L}$ [75] and below 114 $\mu\text{mol/L}$ [76–78], respectively, should be also investigated. Even without metallic catalysts on reduced graphene oxide/graphene oxide-based electrodes, these antioxidants can be easily oxidized at low potentials [79]. Other vitamins present in blood, such as biotin (<3.1 μM) [80], folic acid (<45 nM) [81] or riboflavin (<98 nM) [82] do not require as much attention in selectivity studies due to their relatively low concentration. Neurotransmitter, i.e. dopamine, which can be easily oxidized at a low potential [83] without the need of a certain catalyst [79] are usually also negligible in selectivity studies due to their extremely low concentrations (pM to μM range) [72,84–86]. In blood, there are also unbound amino acids, which could possibly interfere with the analyte by oxidation reaction at relatively high potentials [87]. The concentration of free amino acids in blood varies from <20 μM (i.e., glutamic acid) up to 780 μM (i.e. glutamine) [88]. Thus, if a high oxidation potential is needed for the analyte of interest (>0.5 V vs. Ag/AgCl), a selectivity study should at least take glutamine into account. In addition, although cholesterol is not soluble in water, its concentration in blood is approximately 5.5 mM [89] due to the presence of lipoproteins. Consequently, apart from selectivity studies it is essential to emphasize the importance of anti-biofouling strategies when performing measurements in pure blood or human serum, not only because of the possible interference of cholesterol, but also because of blocking of the electrode due to high protein levels (60–80 mg/mL) [70].

4.1.2. Dermal interstitial fluid

Interstitial fluid, a biofluid akin to blood, has been considered an alternative sample fluid as it can be accessible through minimally invasive means with just a few millimeters beneath the skin, holds great promise for continuous biomolecule monitoring through wearable enzyme-free sensor. In principle, analytes can enter the interstitial fluid in mainly three ways, (i) through the plasma membrane of endothelial cells (transcellular), (ii) by diffusion through the space between cells (paracellular), and (iii) within vesicles through cells (transcytosis) [90]. One crucial parameter in such online-measurements is the lag-time, which denotes the duration from when a rise in blood concentration

occurs to when it is mirrored in the biofluid concentration, i.e., interstitial fluid. The lag time of interstitial fluid varies depending on the patient [5] and the study, typically ranging from 0 to 20 min [91]. It is notable that the commercially available continuous glucose monitoring systems are using interstitial fluid, realized by microneedle electrode systems [92]. The pH present in interstitial fluid is also similar to blood (pH = 7.2–7.4) [70].

Concentrations of analyte, e.g., glucose, cholesterol and lactate in interstitial fluid are highly similar to blood levels [92]. As a result, similar considerations towards selectivity and anti-fouling studies should be performed as for blood, mentioned above. Nevertheless, in comparison to blood the total protein concentration in interstitial fluid is much (13–20 mg/mL) [92], making the measurement in interstitial fluid less prone to biofouling.

4.1.3. Sweat

Sweat is a non-invasive biofluid that provides easy access for sensors, which can be integrated into wearable devices typically placed on the skin [5]. Additionally, interstitial fluid surrounds sweat glands, allowing important analytes present in interstitial fluid to also be found in the sweat [90]. However, the sweat rate varies depending on factors such as the patient's condition, the environmental humidity, the specific body location of the sensor, and the patient's activity level. There are additional challenges associated with sweat-based sensing itself. First, the skin is susceptible to contamination, and old sweat mixing with new sweat can lead to inaccurate result because the changes in analyte concentrations in the new sweat are altered by the presence of the old sweat. Second, the temperature of the sensor is highly dependent on its position on the body, the patient's activity, and the weather conditions. Last, the analyte-concentration levels and pH of the sweat are dependent on the specific body location of the sensor [93].

The pH of sweat typically ranges from 4.0 to 6.8 [70,94] and the lag time between blood and sweat measurements for both ethanol [95] and glucose [96] are approximately 10 min. The sweat-glucose to blood-glucose ratio varies from 0.005 to 0.03, depending on the sweat rate [97]. Notably, a study by Moyer et al. observed a slightly higher sweat-glucose to blood-glucose ratio for increased sweat rates [97]. Despite these variations, changes in sweat-glucose levels do indeed indicate corresponding changes in blood-glucose levels [97]. Calibration by measuring glucose levels in both blood and sweat is however essential to mitigate inaccuracies arising from individual patient differences. Given that glucose concentrations in human sweat are considered low

(ranging from 0.06 to 0.2 mM [98] or in some studies up to 1.11 mM [99]), thus achieving high sensitivity in sweat-based sensor is crucial compared to the sensors developed for measuring in blood or interstitial fluid. Although biofouling is less problematic due to low total protein concentrations in sweat (typically 0.1–0.7 mg/mL) [70], the presence of high metabolite concentrations necessitates a thorough selectivity study. Especially the high concentration of lactate (5–40 mM) [100] and of urea (4–12 mM) [100] highlights the need in investigating the interference of these two biomarkers when ones want to measure glucose in sweat, for instance. Ammonia, a waste product formed by bacteria during protein digestion, is found in sweat (1–8 mM) at higher concentrations than in blood [100]. With that, also ammonia should be part of a selectivity study for non-enzymatic detection in sweat sensors, since it can be oxidized at low potentials by for example core-shell Pt–Ni (OH)₂ nanosheets on Ni foam electrodes [101]. The low concentration of other metabolites like uric acid (~ 25 µM) [102] or ascorbic acid (~ 10 µM) [100] and free amino acids (<13 µM) [100] make them in selectivity studies negligible.

4.1.4. Saliva

Saliva is a non-invasive biofluid that provides easy access for sensors, which can be integrated into pacifiers [103] or mouth guards [104]. Furthermore, saliva can be conveniently used for non-continuous measurements by spitting into a sample collector. The implementation of a sensor into a pacifier is especially relevant for newborns and babies. On average, a normal person produces 1000–1500 mL of saliva per day [5]. However, the secretion of saliva can vary significantly based on the patient's age, diseases or diet. Additionally, the average correlation between blood glucose and saliva glucose levels varies - sometimes better and sometimes worse depending very much on the study and subject (study 1: $R^2 = 0.629$ [105]; study 2: $R^2 = 0.881$ [106]). However, in a study with only one patient, blood and saliva glucose levels were measured at fasting state on different days, a very good correlation between both body fluids was observed ($R^2 = 0.962$) [107]. This indicates the need for individual calibration using both blood and saliva for each patient. Other analytes like cortisol are present in saliva in similar concentrations like in blood and the correlation between both levels seems to be very promising [90], especially since much less interferences are present in saliva compared to blood. Although saliva is a very promising biofluid, studies suggest that patients should fast during measurement to prevent contamination from food or drinks [90]. With a saliva-to-blood concentration ratio of around 1:100 [106], low total protein concentrations (0.2–5 mg/mL) [70], and a pH range between 6.2 and 7.4 [70], prioritizing sensitivity over anti-biofouling is advisable.

Considering a selectivity study, saliva consists of around 99 % of water and the rest are inorganic compounds, such as electrolytes, and organic compounds such as uric acid (~ 200 µM) [108], creatinine (3–400 µM, mean: 11 µM) [109], glucose (0–55 µM) [107], cholesterol (up to 460 µM for patients with hyperlipidemia) [110], lactate (200–600 µM) [111], and polypeptides [112]. Mashazi et al. developed a glucose sensor for saliva and investigated interference caused by sodium chloride, urea, sucrose, fructose, ascorbic acid, uric acid and dopamine at a concentration of 500 µM [113].

4.1.5. Urine

Urine is a non-invasive biofluid that provides convenient access for sensors, which can be integrated into diapers, making it relevant for *in situ* monitoring relevant biomarkers from newborns, babies, or elderly people [114]. Furthermore, collecting a urine sample is painless and straightforward. The pH of urine varies from 4.5 to 8, and it primarily consists of waste substances that the body needs to excrete [70]. However, measuring urine analytes can be challenging due to significant variations in concentration based on factors such as urine volume, sample collection time, and patient characteristics, e.g., gender, age, food intake, medication, and exercise [115]. Additionally, urine analytes may differ in their existing form compared to their counterparts in

blood due to metabolism. To obtain reliable data, it is essential to collect samples from the same patient over an extended period. Considering the lag time of urine is unnecessary since continuous sampling is unlikely.

With over 3000 metabolites identified, urine serves as an excellent matrix since it has the potential to be an indicator for various diseases, especially for diabetes and kidney disorders [115]. However, the abundance of diverse substances in urine can pose significant challenges to non-enzymatic sensors, in particular, in terms of selectivity. Nevertheless, the primary composition of urine includes water (95 %), urea (2 %), creatinine (0.1 %), uric acid (0.03 %), and ions (Na^+ , Cl^- , SO_4^{2-} , NH_4^+ , PO_4^{3-}) which can be taken into account when developed the sensors [115]. For instance, when creatinine is the analyte of interest, researchers like Chen et al. have investigated interfering substances such as uric acid, ascorbic acid, ammonium, and urea. Due to the immense number of metabolites, the choice of additional interfering substances in a selectivity study should involve molecules present in urine that share a similar structure and concentration with specific analytes. Notably, urine has the lowest protein concentration among all mentioned biofluids (below 0.1 mg/mL) [70], eliminating concerns related to antibiofouling.

4.1.6. Breath

Breath serves as a non-invasive sample of the body, offering high potential for early disease detection [116]. Additionally, sensors can be easily integrated into a mask, enabling POC detection or even online measurements [117]. A significant advantage, even in continuous monitoring, is that the biocompatibility of the sensor is less concerned, because, when implemented in a mask, there is no direct contact between the sensor and the patient. The pH of exhaled breath condensate typically ranges from 7.8 to 8.1 [117], and respiratory fluid is believed to have a stable exchange with plasma, with short lag times [118].

Regarding selectivity, exhaled breath primarily contains nitrogen, oxygen, carbon dioxide, water, and various compounds which are also found in blood. However, most of these compounds exist at concentrations 100 to 1000 times lower than in blood [117]. Sakumura et al. identified 63 volatile organic compounds (VOCs) in breath, with 43 of them approaching the limit of detection using gas-chromatography/mass spectrometry [119]. These borderline VOCs can be disregarded in selectivity studies. The remaining VOCs are present at concentrations up to 0.3 ppb (e.g., CH_3CN), between 1 and 5 ppb (e.g., CHCl_3 , CHN , 1-propanol, $\text{C}_2\text{H}_3\text{CN}$, limonene) and between 100 and 200 ppb (e.g., methanol, ethanol, isoprene) [119]. Other VOCs detected include butane, acetone, 2-propanol, C_8H_{16} , dichlorobenzene, $\text{C}_8\text{H}_{17}\text{OH}$, xylene, methylcyclohexane, toluene, and nonanal [119]. Furthermore, non-volatile components such as glucose or peptides are also present [117]. While the average concentration of glucose in respiratory fluid within the lungs is approximately 0.4 mM (diluted by a factor of 12 compared to blood), the concentration in exhaled breath condensate ranges from 0.24 to 5.5 µM [118]. Additionally, low molecular-weight components like ammonia and hydrogen peroxide are found in breath [118]. Ammonia levels can be elevated in exhaled breath condensate due to the high partial pressure of CO_2 , creating an acidic environment that efficiently traps ammonia [118]. However, hydrogen peroxide levels are typically elevated in patients who are suffering from lung cancer and asthma [118]. When studying breath measurements, the focus should primarily be on sensitivity, and considerations related to antibiofouling may be less relevant, since total protein concentration of breath condensate is very low, i.e., at around 1 µg/mL [120,121].

4.2. Non-clinical sample

4.2.1. Water

Water serves as the foundation of human life, and the quality of drinking water significantly impacts human health and well-being. Although the release of pollutants into European water bodies due to

economic activities has decreased over the last decade, there remains room for improvement. Notably, heavy metals releases -such as cadmium (Cd), mercury (Hg), nickel (Ni), and lead (Pb)- have not shown improvement between 2016 and 2021 [122]. However, these heavy metals pose serious health risks even at low concentrations. Beyond Europe, underdeveloped and developing countries face even greater challenges due to lack of strict policies, insufficient capital for expensive waste treatment, and the prevalence of large-scale mining industries. Consequently, water pollution poses a significant problem in these regions.

Given this context, monitoring water pollution becomes crucial for efficient pollutant removal. Pollutants can be categorized into two main classes, i.e., organic pollutants (e.g., antibiotics and pesticides), originating from human and veterinary medicine [123] or agricultural runoff [124], and inorganic pollutants (e.g. Cd, Hg, Ni, Pb, chromium (Cr), and arsenic (As) ions), usually caused by industrial processes [125]. Additionally, several other parameters warrant measurement, including pH, nitrogen-containing molecules (ammonia, nitrate, and nitrite), water hardness, dissolved oxygen levels, disinfectants (such as free chlorine or hydrogen peroxide), and sulfide/sulfite content [126]. Furthermore, the presence of microplastic caused by rising plastic waste in water has become increasingly more relevant due to their potential health impacts. A study by Goodman et al. demonstrated the need of comprehensive microplastic monitoring, as microplastic intake can adversely affect kidney and liver function, thereby impacting human health negatively [127].

In the field of toxic metal ion detection, selectivity and anti-biofouling studies depend on the specific water being analyzed. Cho et al.'s review highlights typical ions studied for selectivity, including Cu (II), Fe(II), Fe(III), Ni(II), Zn(II), Cr(III), As(III), Sb(III), Se(IV), Pb(II), Al (III), Fe (III), Ni (II), Co (II), fluoride (F^-), thiocyanate (SCN^-), iodide (I^-), phosphate (PO_4^{3-}), sulfate (SO_4^{2-}), nitrate (NO_3^-), sodium (Na^+), calcium ($Ca(II)$), magnesium ($Mg(II)$), potassium (K^+), and carbonate (CO_3^{2-}) [126]. Additionally, investigations have explored the interactions of benzene, xylene, surfactants, and ethylenediaminetetraacetic acid (EDTA) with analyte metal ion [126].

Altahan et al. developed a non-enzymatic sensor for ammonium in water and tested its selectivity against interfering ions such as Na(I), Ca (II), Mg(II), nitrate, phosphate, F(-I), Cl(-I), formate, acetate, oxalate and β -phthalate [128]. Furthermore, they measured the recovery after spiking tap and mineral water samples with ammonium [128]. For such cases, anti-biofouling studies are not needed due to the expected low amount of proteins in the real samples.

Considering pesticides, especially organophosphorus pesticides (OPPs), which are derivatives of phosphoric, phosphinic, phosphonic acids, or phosphorothionate, are very popular due to their efficiency, selectivity, and fast degradation [13]. However, OPPs pose significant ecological and health risks, necessitating the development of effective detection methods [13]. Due to the low maximum residue limits of OPPs (ranging from 0.01 to single-digit ppm concentrations, depending on the country), achieving good selectivity through direct electrochemical detection is challenging [13]. This is because fruits and vegetables contain many antioxidants in high concentrations, which, due to their function as antioxidants, have low oxidation potentials. Furthermore, non-enzymatic sensors offer hardly the ability to distinguish between structurally similar organophosphorus pesticides. Therefore, affinity-based approaches such as molecularly imprinted polymers (MIPs) seem to be more promising [129].

4.2.2. Food and beverages

Food and beverages play a crucial role in our daily lives, and ensuring their safety and quality is essential. Just as water quality affects human health, the composition of food and beverages can significantly impact consumers. Common analytes in food and beverage samples include contaminants [130] such as hydrazine (N_2H_4), malachite green, and bisphenol A), additives [130] (like ascorbic acid, caffeine, caffeic

acid, sulfite, and nitrite), inorganic pollution (as discussed in chapter 4.2, water), pesticides (categorized into insecticides, miticides, herbicides, nematocides, fungicides, molluscicides, and rodenticides) [131], pathogens [132] such as *Escherichia coli*, allergens [132] (e.g., gliadin, a protein component of gluten), and toxins [132] such as botulinum toxin. The vast majority of complex analytes highlights the need for affinity elements, including antibodies, aptamers, and molecular imprinted polymers (MIPs) [131]. In this review, we focus on MIPs as an affinity element since they are cheaper to produce and can be very stable, depending on the monomers used [133]. Furthermore, antibodies and aptamers inherit similar drawbacks to enzymes (e.g., sterilization ability, long-term storage, environmental stability) [131,134,135].

Regarding antibiofouling and selectivity studies, given the wide variability in sample matrices, it is crucial to recognize that generalizing findings across all samples may not be appropriate. However, one approach we recommend for such studies is to measure the analyte in the real matrix of the final application (which is of course also essential for other matrices than food and beverage). Analyzing the analyte within the actual matrix of its intended application provides insights into real-world behavior, accounting for potential interferences and matrix effects. Researchers can spike the sample with the analyte at various concentrations and investigate reproducibility and recovery. Additionally, exploring structurally related compounds, especially those with similar applications, allows us to assess cross-reactivity and specificity (for example, investigating other pesticides when an insecticide is the analyte) [136]. However, it is important to note that diluting the real matrix with a buffer is acceptable, but extreme dilution can distort results and is prone to cause errors especially when applied to analytes with extremely low concentrations. Researchers should aim for a dilution factor within the range of 1–10 to maintain relevance. Many recovery studies have reported great recovery rates. However, it should be noted that many of these studies typically performed sample dilution prior to spiking the analyte of interest. Such experiment does not well-reflect the real effects of matrix that has on the spiked analyte. Instead, the analyte should be spiked into undiluted samples, and later perform dilution to eliminate interfering effects from the food or beverage matrices.

4.2.3. Cell culture medium

Monitoring substrate consumption and product generation of bioreactors in a precise and, ideally, real-time manner is crucial in controlling productivity and product quality [137]. Non-enzymatic electrodes are highly promising and practical in this area owing to their low cost and superior stability under common sterilization techniques. Bioreactor typically contains cell culture media that play a pivotal role in preserving, amplifying, and differentiating various cell types for bio-manufacturing products of interest. Cell culture media are essential for maintaining and growing cells *in vitro*, providing an artificial environment that simulates the natural conditions for cultured cells. The main tasks of cell culture media include supplying energy sources to the cells, maintaining proper salt balance and pH for a healthy cell growth, and facilitating the removal of cellular waste products.

Cell culture media typically contains well-defined composition. For example, a typical *E.coli* culture medium, namely LB-Bouillon (Lennox; Sigma Aldrich), contains 5 g/L NaCl, 10 g/L tryptone, 5 g/L yeast extract. It is buffered between a pH of 6.8–7.2 (usually using a phosphate buffer). Additionally, glucose, a crucial energy substrate, is added to cell culture media in concentrations, typically ranging from 5 to 25 mM. The typical high concentration of substrate makes the development of highly sensitive non-enzymatic sensors less concerned. However, a number of electroactive species in the culture media can potentially generate interfering signals which have to seriously take into account for selectivity studies. For example, tryptone and yeast extract contribute a variety of amino acids, e.g., glutamic acid, aspartic acid and lysine, in relative high concentrations, and vitamins, e.g., B₁, B₂, B₆, nicotinic acid, biotin, pantothenic acid, and folacin [138]. Furthermore, yeast

extract provides a rich source of proteins, emphasizing the need for anti-biofouling studies, in particular for online-monitoring purpose. It is also plausible to develop *in situ* cleaning procedure to recovery non-enzymatic electrode' functionality during operation. An overview of the various sample matrices discussed in this chapter is given in Table 3.

5. Advances in molecular imprinting technology towards selective POC non-enzymatic EC sensors

Any enzyme-free sensing strategy has to strike a balance between catalytic efficiency and selectivity for the targeted analyte. Various nanomaterials have been developed in the past decades with their (electro-)catalytic properties approaching those of enzymes. Likewise, molecular imprinting has been used to increase the selectivity of detection. Molecularly imprinted polymers are produced by a synthesis strategy that includes the target analyte, or a highly resembling

chemical species, as a template during the polymerization. The template molecule is added in an approximately stoichiometric proportion to the functional monomer(s) of the pre-polymerization mixture. These monomers are selected to show significant, but usually non-covalent interactions with the template molecule, e.g. by the formation of hydrogen bonds. Hereby the template is entrapped within the growing polymer segments, and, after it has been washed out of the solid polymer, leaves nanopores with a "molecular memory" behind. These nanopores will preferentially bind to the molecules that were used as templates, even in the presence of interfering molecules of a similar size, and can be used as artificial receptors or "plastic antibodies" in chemical sensors. While classical molecular imprinting technology deals with bulk polymers, e.g. 3D-materials, non-enzymatic electrochemical sensors often rely on thin films (thicknesses in the nanometer range) or surface imprinting approaches. Several recent reviews cover the rapid progress in the field: Ahmad et al. and, more recently, Li et al. focus on electrochemical MIP-based sensors [139,140]. Crapnell et al., Saylan

Table 3
Sample matrices, their properties, and considerations for enzyme-free sensor development.

Matrix (pH)	Relevant compound (concentration)	Advantages	Disadvantages	Concerns for enzyme-free sensors development
Clinical sample The following are the Supplementary data related to this article:				
Blood (7.3–7.4)	- Glucose (3.9–5.6 mM) - Urea (~ 5 mM) - Lactate (<2.2 mM) - Uric acid (~ 0.5 mM) - Ascorbic acid (~ 0.1 mM) - Free amino acids (0.02–0.78 mM) - Cholesterol (5.5 mM) - Total protein (60–80 mg/mL)	- High abundance of analytes - High accuracy	- Invasive - High protein and interference concentration	- Selectivity - Antibiofouling
Interstitial fluid (7.2–7.4)	Similar to blood -Total protein (13–30 mg/mL)	- Continuous monitoring -Wearable devices	- Minimal invasive	- Selectivity - Antibiofouling - Lag time (0–20 min)
Sweat (4.0–6.8)	- Glucose (0.06–0.2 mM) - Lactate (5–40 mM) - Urea (4–12 mM) - Ammonia (1–8 mM) - Total protein (0.1–0.7 mg/mL)	- Continuous monitoring - wearable devices - Non-invasive	- Many factors that influence individual sweat rate	- Sensitivity - Selectivity - Body location of sensor - Lag time (~ 10 min) - Correlation between blood and sweat level
Saliva (6.2–7.4)	- Glucose (<0.055 mM) - Uric acid (0.2 mM) - Creatinin (<0.4 mM) - Cholesterol (<0.46 mM) - Lactate (0.2–0.6 mM) - Total protein (0.2–5 mg/mL)	- Non-invasive - Continuous monitoring - Sensor integrateable in pacifier (newborn diagnostics) - low amount of interferents	- Many factors that influence secretion of saliva - Contamination from food and drinks	- Sensitivity - (Selectivity) - Lag time - Correlation between blood and saliva level
Urine (4.5–8.0)	- Urea (2 %) - Creatinine (0.1 %) - Uric acid (0.03 %) - Total protein (0.1 mg/mL)	- Non-invasive - Sensor integrateable in diapers - low protein content	- Continuous monitoring is not possible -many factors that influence concentrations	- Sensitivity - (Selectivity) - Sample should be taken over a longer periode
Breath (7.8–8.1)	- Glucose (0.005 mM) - Volatile organic compounds - Ammonia - Hydrogen peroxide - Lactate - Total protein (0.001 mg/mL)	- Non-invasive - Sensor integrateable in mask - Continuous monitoring - low protein content		- Sensitivity - (Selectivity)
Non-clinical sample				
Water	- Heavy metals - Antibiotics - Pesticides - Fertilizer -pH	- Less fouling	- Many possible interferences - Hard to be selective	- Sensitivity - Selectivity
Food and beverages	- Contaminants - Additives (Vitamins) - Pesticides - Allergens - Toxins -pH	- Usually, matrix is very well known	- Many possible interferences - Hard to be selective	- Sensitivity - Selectivity - Fouling
Cell culture medium	- Glucose (5–25 mM) - Phosphate - Amino acids - Vitamins - pH	- Very defined compositions	- Too high conc. - High concentrated interferences (Tryptone (10 g/L); Yeast extract (5 g/L))	- Selectivity - Fouling

et al. and, more recently, Ni et al., summarize recent advances in MIP-based electrochemical sensors for diagnostic biomarkers and medical applications [141–143]. Mazzotta et al. reviews MIP-based protein sensors [144]. Lowdon et al. covers the use of MIPs for commercial applications in low-cost sensors [145]. Caldara et al. and, more recently, Hernández-Ramírez et al. highlight the use of MIPs for non-enzymatic glucose sensing [146,147], while Zhou et al. reviews specifically the field of wearable (enzymatic and non-enzymatic) electrochemical sensors for tear glucose detection with a focus on the nanomaterials used [148]. Murugesan et al. review the field of MIP-based electrochemical cholesterol sensing [149]. Some key recent examples of “reagent-less”

electrochemical MIP-sensors (e.g. MIPs with built-in signal transduction without the need for externally added reporter molecules like ferri-/ferrocyanide) will be highlighted in the following section. The summary of these examples, with the targeted analytes and the used real sample matrices, is given in Table 4.

Cho et al. demonstrated highly selective direct oxidation of glucose on hierarchical CuCo dendrite bimetal, coated with a glucose-imprinted polymer from Nafion, polyurethane and aminophenyl boronic acid [150]. The sensor was shown to selectively detect glucose in the presence of other monosaccharides (e.g. mannose, fructose) and electrochemical interferents like uric acid and acetaminophen. Furthermore,

Table 4

Summary of molecular imprinting technology towards selective POC non-enzymatic EC sensors.

Electrode/MIP	Transduction principle	Operating pH	Analyte	LOD	Interference species	Sample matrices	Ref.
SPCE/CuCo/Nafion-PU-APBA	catalytic reaction	pH 7.4 (with <i>in situ</i> OH [−] generation)	glucose	0.65 ± 0.10 μM	uric acid, acetaminophen, dopamine, ascorbic acid, L-cysteine, and other saccharides	artificial and whole blood	[150]
HOPG/Nafion/GOD/NiCO ₂ O ₄ @Fe ₃ O ₄ /DVB/Tris(4-vinylphenyl) boroxine	catalytic reaction	pH 7.2 (PBS) and NaOH (0.1 M)	glucose	0.05 μM	mannose, allose, altrose	not tested	[151]
bipolar SPEs on PE-paper/PANI	resistance changes	pH 7 (DI water)	glucose	1.0048 mM (DI water) and 1.1713 mM (bovine blood)	not tested	spiked bovine blood solution	[152]
GCE/rGO-β-CD/PPy-HCF	current changes by embedded redox marker	PBS (pH 7.4)	cortisol	19.3 pM	testosterone, progesterone, cholesterol, lactate, glucose, urea	artificial saliva	[156]
Carbon-coated NCD/NOBE	impedance changes	PBS (pH 7.4)	testosterone	0.5 nM	estriol, β-estradiol	spiked urine and saliva	[157]
GCE/AuNP@Fe-BDC/N,S-GQD/PPy	current changes in presence of a redox probe	pH 7.0	histamine	0.026 nM	transition metals (Cu ²⁺ , Cd ²⁺ , Zn ²⁺ , Pb ²⁺ , Na ⁺ , K ⁺ , Mg ²⁺ , Cl [−] , SO ₄ ^{2−}), dopamine, uric acid, ascorbic acid, glutathione, serotonin, tyramine, histidine	spiked human serum and canned tuna fish	[158]
SPCE/PANI-AF	impedance changes	pH 7.4 (PBS)	tryptophan	8 pM	tyrosine, phenylalanine	spiked milk, cancer cell media	[159]
GCE/GNP/polydopamine	impedance changes	pH 7.4 (PBS)	creatinine	0.02 pg/mL	glycine, sarcosine, urea, glucose, uric acid, bilirubin, creatine, cholesterol, lactic acid, ascorbic acid	spiked Human serum, urine, and peritoneal dialysis fluid	[160]
Filter paper coated with carbon paint/rGO/AA/EGDMA	potentiometric changes	pH 7.5 (PBS)	LOS-K	0.27 ± 0.03 μM	paracetamol, ascorbic acid and dextromethorphan	pharmaceutical formulations and in spiked human urine samples	[161]
GCE/Ag-NP@Cu-BDC/N-CNT/PPy	current changes by embedded redox marker	pH 7.5 (PBS)	oxaliplatin	0.016 ng/mL	transition metals (Cu ²⁺ , Cd ²⁺ , Zn ²⁺ , Pb ²⁺), Na ⁺ , K ⁺ , Mg ²⁺ , Cl [−] , SO ₄ ^{2−} , dopamine, uric acid, ascorbic acid, glutathione, 5-fluorouracil, capecitabine, cisplatin, satraplatin, flutamide, carboplatin, doxorubicin	pharmaceutical injections, human plasma, and urine samples	[162]
GSPE/o-PD	change in impedance in presence of a redox probe	pH 7.4 (PBS)	VEGF	0.08 pg/mL	HER2, CA125; PSA, MUC16	spiked Human serum	[163]
SPCE/2-aminophenol	change in impedance in presence of a redox probe	pH 7.4 (PBS)	galectin-3	range of 0.50 ng/mL and 5.0 μg/mL	glucose, creatinine, BSA, CA 15-32	spiked human serum	[164]
SPCE/PPy/carboxylated pyrrole	change in impedance in presence of a redox probe	pH 6.0 (PBS)	IL6	0.02 pg/mL	not mentioned	spiked human serum	[165]

SP(C)E: screen-printed (carbon) electrode; PU: polyurethane; APBA: aminophenyl boronic acid; HOPG: highly oriented pyrolytic graphite; GOD: glucose oxidase; DVB: Divinylbenzene; PE: polyester; PANI: polyaniline; DI: deionized; GCE: glassy carbon electrode; rGO: reduced graphene oxide; CD: cyclodextrin; PPy: polypyrrole; HCF: hexacyanoferrate; NCD: nanocrystalline diamond; NOBE: *N,O*-bismethacryloyl; AuNP: gold nanoparticle; Fe-BDC: Fe metal-organic framework; GQD: graphene quantum dot; AF: lysozyme amyloid fibril.

GNP: graphene nanoplatelet; LOS-K: losartan potassium drug; AA: acrylamide; EGDMA: ethylene glycol dimethacrylate; N-CNT: nitrogen-doped carbon nanotube; GSPE: graphite screen-printed electrode; o-PD: *ortho*-phenylenediamine; VEGF: vascular endothelial growth factor; HER2: human epidermal growth factor receptor 2; CA125: carbohydrate antigen 125; PSA: prostate specific antigen; MUC16: mucin 16; BSA: bovine serum albumin; IL6: Interleukin 6.

the authors have proven the reliability of the proposed sensors for determination of glucose in whole blood samples that collected from seven healthy volunteers. The obtained values from the sensors were in good agreement with the ones obtained from using commercially available glucometer in which a paired *t*-test was performed to confirm their insignificant differences. Chen et al. prepared catalytically active NiCo₂O₄-nanomaterial with sea urchin morphology, coated with a glucose-selective MIP, and doped with Fe₃O₄ nanoparticles for the detection of glucose at alkaline pH [151]. Glucose could be detected with a higher selectivity than mannose, allose and altrose. Chen et al. demonstrated a paper-based MIP glucose sensor [152]. The low-cost design, without a reference electrode, is based on the detection of resistance change between bipolar electrodes, covered with an imprinted polyaniline layer. A linear detection range between 2 and 11 mmol/L glucose with high signal correlation (0.984) was obtained in real bovine blood samples, emphasizing the potentiality of MIPs in complex biological sample. Garcia-Cruz et al. demonstrated a novel type of electro-responsive, imprinted nanoparticles, coined “eNanoMIPs” [153]. The ca. 250 nm sized spherical particles are produced by a highly standardized and scalable workflow, are tagged with a polymerizable ferrocene derivative and can be covalently attached to electrodes. By their intrinsic signaling properties upon target molecule binding, direct electrochemical DPV detection is possible. Glucose detecting eNanoMIPs-based sensors have been produced and showed a linear dose-response at 0.5–1.5 mmol/L glucose and sufficient selectivity towards fructose, maltose and lactose. A dip-stick MIP sensor for glucose with a high selectivity for glucose was recently reported by Caldara et al. [154]. Glucuronic acid was used as a dummy template, acrylamide as the functional monomer and EGDMA as crosslinking monomer. The resulting bulk imprinted polymer was ground to small particles, mixed with a commercial graphite ink and used for the screen-printing of electrodes. The binding of glucose resulted in changed thermal resistance and electrochemical impedance of the electrode material, allowing for heat-transfer measurement (HTM) or EIS to be used for signal transduction. Glucose was detected in urine between 0.05 and 0.33 mmol/L, with a LOD of ca. 1.4 µmol/L, while the potentially interfering saccharides fructose, sucrose and lactose did not produce significant signals. A different approach was taken by Okhokhonin et al. who designed an electrocatalytic glucose sensor by modifying carboxylated MWCNT with Ni(II)acetoacetate and coated these with a PEI layer [155]. Molecular imprinting was achieved by adding another PEI layer on top, which was crosslinked in the presence of 10 mmol/L glucose (for the MIP) or without glucose (for the NIP). The purpose of the top PEI layer was to act as a diffusion barrier towards the electrode. The sensor showed high electrocatalytic currents in the presence of glucose, allowing for its detection in the range between 0.14 and 10 mmol/L glucose in alkaline solution, while the corresponding non-imprinted control material did not react to glucose. Next to glucose, cholesterol is one of the most important small molecular metabolites in point-of-care diagnosis. Murugesan et al. have recently reviewed the field of electrochemical biosensors for cholesterol based on MIPs [149].

Steroid hormones are another example of a small molecule biomarker. Cortisol in saliva is considered the gold standard for stress monitoring. In contrast to glucose, the relevant concentration range is in the nanomolar range. Goyal et al. built a sensor based on cortisol imprinted polypyrrole (PPy), doped with ferricyanide during electropolymerization, and coupled to reduced graphene oxide functionalized with β-cyclodextrin (β-CD) as the transducer [156]. Cortisol was detected in picomolar to nanomolar concentrations in buffer and artificial saliva without any added reagents. The sensor showed preferential selectivity towards cortisol vs. other steroid hormones. Increased testosterone levels are indicative of some cancer types and doping in sports. Kellens et al. used micro-patterned molecularly imprinted polymer structures on functionalized nano-crystalline diamond-coated substrates for testosterone detection [157]. N,O-bismethacryloyl ethanolamine was synthesized and used as the functional monomer.

Concentrations between 0.5 and 20 nmol/L could be detected with an EIS transducer in buffer/ethanol and urine/ethanol mixtures. The presence of relatively low testosterone concentrations in urine and saliva samples still necessitates sample preparation steps, e.g., filtration or pretreatment, to remove large molecular impurities that potentially hinder the binding of testosterone to MIP binding pockets. However, the study did not validate their approach with standard method, e.g., commercially available enzyme-linked immunosorbent assay.

Mahnashi et al. detected the allergy related messenger histamine with a novel hierarchical nanomaterial, gold nanoparticle functionalized Fe-metal organic framework (Fe-BDC) and nitrogen-sulfur co-doped graphene quantum dots (N, S-GQDs) [158]. A high selectivity was obtained by histamine-imprinted polypyrrole electropolymerized on the gold nanoparticles and histamine could be measured in human serum between 0.026 and 250 nmol/L with excellent recovery (98.5–102.5 %). Furthermore, the authors demonstrated the ability of the sensors in measuring spiked histamine in tuna fish extract also with good recovery (97.2–102.1 %). Here, the authors also validated their sensors with the UHPLC-MS/MS and found no significant difference between the two approaches, supporting the sensor's reliability. Nevertheless, extensive sample preparation steps were required in this study. Alam et al. demonstrated the highly sensitive detection of tryptophan (10 pmol/L – 80 µmol/L) by a polyaniline film chemically polymerized (in the presence of tryptophan) onto lysozyme amyloid fibril-based material [159]. The novel nanomaterial offers high tensile strength and a large surface area and acted as a dopant for polyaniline at the same time. Tryptophan was detected in 10-fold diluted milk and undiluted cancer cell fluid with an impedimetric sensor. The values of tryptophan obtained from both samples (n = 5) using the sensors were highly comparable with the results shown by HPLC (relative % errors less than ca. 2). An ultra-sensitive creatinine MIP-sensor was presented by Li et al. [160]. A LOD of 0.02 pg/mL and a wide detection range up to 10⁹ pg/mL was achieved. Small molecule drugs were also used as targets. Hassan et al. have developed a novel paper-based, low-cost potentiometric sensor for the pharmaceutical drug losartan using a molecular imprinting approach [161]. While it is intended as a low-cost potentiometric sensor, the sensing material showed high selectivity and sensitivity also with other detection modalities like EIS and was used to detect losartan and its metabolites in urine samples. The measurement of spiked losartan in an undiluted urine sample exhibited a good recovery (n = 3), indicating the as-generated MIP for losartan was not affected by the interferences existed in the urine. This may be possibly due to the fact that the concentrations were in micromolar ranges.

The cytotoxic cancer drug oxaliplatin was the target analyte for Mahnashi et al. [162]. Polypyrrole was electrodeposited on a GCE modified with silver nanoparticles functionalized Cu-metal organic framework (Cu-BDC) and nitrogen-doped carbon nanotubes (N-CNTs). The combination of N-CNTs and Ag@Cu-BDC improves both the conductivity and provides the anchoring sites for the polymer film. A linear range of 0.056–200 ng/mL was obtained by a DPV detection scheme and real urine samples were successfully analyzed.

Macromolecular targets like protein biomarkers require a different molecular imprinting strategy than small molecules. One successful approach relies on thin polymer films or (core-shell) nanoparticles, that are “surface imprinted”. Usually, the template macromolecules are immobilized at the surface and a thin polymer film is deposited onto it. The thickness of this film is on the order of the macromolecular templates, thus avoiding large mass transport resistances and adverse steric effects. Along these lines, Bozal-Palabiyik et al. have created a single-use MIP- biosensor for the tumor marker VEGF [163]. Non-conducting poly (o-phenylenediamine) was electropolymerized onto screen-printed graphite electrodes in the presence of the template VEGF. VEGF was detected in the relevant range from 20 to 200 pg/mL with a LOD of 0.08 pg/mL. Here, filtered and diluted human serum (1:20 dilution in PBS) was spiked with VEGF protein for studying the effect of sample matrix. The authors achieved a good recovery rate (90–110 %, n = 5) with

moderate analyte concentrations, i.e., 30, 60, and 120 pg/mL. Cerqueira et al. published their work on a sensor for the tumor marker galectin-3 (Gal-3) [164]. They used 2-aminophenol as the functional monomer and obtained a detection range from 0.5 ng/mL to 5000 ng/mL Gal-3 in spiked serum using EIS for signal transduction. The detection of Gal-3 in undiluted spiked sample was less sensitive than in PBS ca. 1.5-times. It should be also noted that when the sensors were exposed to the spiked sample the signals of non-imprinted polymer surface also increased in comparison to PBS, indicating higher tendency of non-specific binding from interfering molecules. Goncalves et al. developed a sensor for the Alzheimer's disease marker interleukin-6 (IL-6) using a co-electropolymerization approach [165]. Pyrrole (Py) and carboxylated pyrrole were used as monomers. The design used a screen-printed electrode and EIS and they obtained a LOD of 0.02 pg/mL in spiked serum samples. These works illustrate that there does not seem to be a "golden rule" for the molecular imprinting of biomarkers. A large variety of functional monomers and nanomaterials were combined to achieve the best possible combination of characteristics. This variety, on the other hand, may be a barrier for the broad commercial application of MIP-based diagnostic products. In spite of promising analytical performances and innovative low-cost designs, none of the presented MIP-based POC sensors has yet been compared to existing state-of-the-art POCT devices in a clinical study. This will be a necessary step to commercialization and achieving a broader acceptance of the technology.

6. Other challenges and promising studies

6.1. Anti-fouling

Fouling, the non-specific adsorption of biological materials such as proteins (biofouling) or reaction products, poses significant challenges in non-enzymatic sensors. In POC applications, minimizing sample treatment is crucial to reduce errors associated with additional processing steps and to simplify detection. The goal is to measure analyte of interest in the presence of these fouling molecules without any influence or minimal disturbance from them. To achieve this, effective antifouling strategies are essential, ensuring accurate and reliable measurements especially in complex biological environments. Antifouling strategies include the use of surface polymer coatings [166–170] (e.g., electro-neutral, hydrophilic polymers such as PEG, zwitterionic polymers, or conducting polymers), hydrogels [168,169,171], biomolecules such as peptides [166,168,169] or proteins [169], nanoporous membranes [170,171], and self-assembled monolayers [166–168,170–172] (e.g., thiols on gold surfaces). For example, Moonla et al. applied a layer of chitosan and poly(vinyl chloride) (PVA) onto their microneedle working electrode using a drop-coating technique [173]. This layer reduced biofouling during continuous ketone measurements in human interstitial fluid. Here, the chitosan and PVA layer minimized electrode fouling by acting as semipermeable and permselective outer layers, respectively. Although the strategy has been applied for enzyme-based biosensor, it is promising for non-enzymatic sensors as well. Additionally, Shin et al. applied a conductive PEG-PEDOT hydrogel, which ensured the sensor's non-fouling properties even in bovine blood diluted 1:1 in PBS [174]. They photopolymerized a PEG hydrogel on an ITO electrode and then electropolymerized PEDOT. In this setup, PEDOT within the hydrogel coating served as an electrochemical transducer. Furthermore, Zhu et al. utilized a branched-shaped zwitterionic peptide on electrodeposited gold nanoparticles to enhance electron transfer and antifouling properties [175]. The biosensor exhibited excellent stability in wastewater, retaining 91.8 % of its initial signal after 15 days.

Apart from surface coatings, an electrochemical cleaning step can be used before subsequent measurement to remove adsorbed molecules [170]. Additionally, the composition of the catalyst can influence the adsorption energy of the reaction product, thereby affecting the fouling caused by the analyte itself. This has been proven by Xi et al. who

showed that through density functional theory calculations that the reaction product of hydrogen peroxide reduction binds more strongly to pure platinum nanoparticles compared to Pt–Ni alloyed nanoparticles, leading to a significant increase in the reaction rate when the bimetallic alloy was used [176].

6.2. Measurements performed under physiological conditions

Often, enzyme-free reaction mechanisms are highly pH-dependent and do not work under physiological conditions (see also section 2). For example, glucose only reacts with certain catalysts in an alkaline medium [177]. However, some catalysts do work under neutral conditions, but they often consist of expensive materials such as Au/Pt alloys or require complex synthesis strategies, such as creating core-shell structures [178]. Furthermore, not only the catalyst but also the carbon matrix plays an important role. Mei et al. observed that PtNi nanoparticles could oxidize glucose at physiological pH when the particles were attached to multi-walled carbon nanotubes, but they observed no catalytic effect when a pristine carbon black sample was used as the matrix [27]. Hence, the question of whether a catalyst can oxidize the analyte under physiological conditions may be more complex than expected, and strategies to adjust the pH on the catalyst surface seem to be very useful. In this regard, researchers have proposed various strategies. For example, Zhu et al. used an Ecoflex™ porous rubber membrane containing 0.05 mM NaOH as a layer on top of the electrode to provide an alkaline environment [179]. The authors successfully demonstrated the practical utility of the porous membrane integrated microfluidic non-enzymatic glucose sensors in sampling sweat and detecting glucose in sweat [179]. Alternatively, Strakosas et al. exploited an electrode containing Pd nanoparticles to generate hydroxide ions at -1.0 V (vs. Ag/AgCl) [180]. These ions diffused to the closely placed cobalt-oxide working electrode, which, at the reduced local pH, was capable of oxidizing glucose at $+0.5$ V [180]. In a similar manner, Zhu et al. used a gold rod as a working electrode and applied a potential of -2.0 V for 20 s (vs. a polypyrrole-coated Pt quasi-reference electrode) to increase the local pH on the working electrode and subsequently oxidized glucose at $+0.2$ V [181]. After that, a potential of $+1.0$ V was used to clean the electrode surface, enabling nonenzymatic wearable sensor for continuous real-time monitoring of perspiration glucose during physical activities [181].

6.3. Biocompatibility

Since non-enzymatic electrochemical sensors contain reactive and nanometric-sized catalysts, biocompatibility needs to be considered, even though the catalyst material itself may be macroscopically safe, such as noble metals. Especially for continuous measurements where the sensor, for example, directly touches the patient's skin over weeks, the safety of the product needs to be ensured by minimizing possible adverse reactions such as inflammation or toxicity. Biocompatibility also maintains the functionality of devices in preventing immune responses from the patient. Thus, biocompatibility is not only essential for safety and the patient's well-being but also enhances the longevity and stability of devices, making them suitable for long-term use. Furthermore, regulatory compliance needs to be considered to gain approval for clinical use. In the literature, several approaches have been proposed to achieve or prove biocompatibility of electrode materials. For example, Dang et al. tested the biocompatibility of their Prussian blue (PB) nanoparticles intercalated Ti_3C_2 nanosheets biosensor by conducting cytotoxicity assays using L292 mammalian fibroblast cells [182]. Cells were co-cultivated with various concentrations of the sensor components, i.e., PB, Ti_3C_2 , and PB/ Ti_3C_2 [182]. The cytotoxicity was assessed using the MTT method [183]. The authors have proven that the PB/ Ti_3C_2 did not cause significant cytotoxicity to the investigated skin cells for 48 h [182]. They further demonstrated the real-time and *in situ* detection of H_2O_2 secreted from living HeLa cells using glassy carbon electrode

modified with PB/Ti₃C₂ [182]. Besides the *in vitro* study shown by Dang et al., Chen et al. recently developed a non-enzymatic glucose sensor for sweat by incorporating gold nanoparticles onto aminated multi-walled carbon nanotubes as a catalyst [184]. The material was cross-linked in a carboxylated styrene-butadiene rubber and PEDOT:PSS matrix, which was consecutively dropped-cast onto a screen-printed electrode [184]. Biocompatibility was demonstrated by observing no allergic reactions or skin irritations after 48 h of contact with a volunteer's skin [184].

6.4. Long-term stability and storage conditions

In sensor development, studying the long-term usability of a sensor is crucial as it enables continuous monitoring. Continuous monitoring provides comprehensive data on a patient's health, detecting short-lived but significant health events that single measurements might miss [185]. Additionally, it reduces the impact of temporary fluctuations, allowing for a more accurate determination of the patient's health status [185]. Therefore, investigating the aging of electrodes during long-term measurements is essential, ideally identifying and preventing its causes. Furthermore, examining the storage conditions of a sensor and the effect of aging is vital if the sensor is to become a viable product. Several studies in the literature address long-term measurements and aging during storage. For example, Li et al. demonstrated that freshly prepared graphene/graphite is more hydrophilic than traditionally expected [186]. The adsorption of hydrocarbon contaminants from the air increases hydrophobicity [186]. In addition, Behrent et al. investigated the aging of LIG electrodes under various conditions [187]. They found that storage environment such as the container (glass or plastic) and sources of hydrocarbon contaminants, e.g., glue or nail polish used to insulate the electrode, significantly impacted the electrochemical performance and contact angle during aging [187]. These examples highlight the need for effective strategies in protecting LIG surface after scribing. Here, Zhang et al. electrodeposited gold on a LIG electrode and further coated it with chitosan [188]. The super hydrophilic Chitosan-Au-LIG showed superior performance not only after storage in ambient conditions (bare LIG: 90 % decrease in redox peak currents after 30 days; Chitosan-Au-LIG: 3 % decrease in redox peak currents after 30 days) but also after reuse [188]. While bare LIG electrodes lost 33 % of redox peak currents in a second measurement one day later, Chitosan-Au-LIG only lost 5 % of performance after 10 consecutive days with a measurement each day [188].

6.5. Mobility and placement

In real-life scenarios, the use of commercial reference and counter electrodes, such as an Ag/AgCl-reference electrode or a platinum wire as a counter electrode often presents mobility challenges and restricts the possible sensor placement locations. Consequently, it becomes crucial to explore alternative approaches with high reliability. One such approach involves testing the material of the working electrode itself as a counter electrode or even using it as a reference electrode. By doing so, the stability of the produced pseudo reference electrode can be investigated by measuring its open circuit potential versus a commercial reference electrode [83]. Notably, printed electrodes offer a convenient solution. In a printed 3-electrode system, all three electrodes can be placed next to each other on a planar surface, simplifying handling, ensuring always the same distance between the electrodes to enhance reproducibility, and reducing overall system complexity. This streamlined design also enhances cost-effectiveness and facilitates mass production.

Considering wearable sensors, the comfort of the user is paramount. The device should be lightweight, flexible, unobtrusive, and easy to wear for extended periods. Furthermore, they should be mechanically stable and have a long lifespan, particularly for wearable devices that may be exposed to various environmental conditions and physical movements.

Especially when using the most common measurement techniques,

such as chronoamperometry, cyclic voltammetry, differential pulse voltammetry, and square wave voltammetry, a battery-less NFC potentiostat offers significant advantages with comparable performance to commercial benchtop potentiostats [189–191]. These potentiostats are approximately the size of a credit card and are affordable [189,190]. The wireless power supply operates through inductive coupling between an NFC-capable smartphone and the potentiostat. The primary coil (smartphone) generates a magnetic field, while the secondary coil (potentiostat) receives energy [192]. This enables devices to charge or power up without physical connections at distances of up to 5 cm [192]. Additionally, communication between the potentiostat and the smartphone is based on electromagnetic induction [192]. However, there are limitations in the potential ranges that can be used due to the NFC technology's limited power supply, which can be addressed through sensor miniaturization [189].

6.6. Efficiency, cost, and simplicity

Electrochemical sensors play a crucial role in rapid and efficient analyte detection, especially when working with minimal sample volumes. To achieve cost-effectiveness, it is advisable to produce electrodes from inexpensive raw materials, such as polymers or paper, rather than relying on, for example, commercial screen-printed electrodes as the foundation for the electrode system. This approach not only reduces overall costs but also minimizes dependence on external suppliers.

When designing the production process, consider energy efficiency. Avoid energy-intensive steps (such as heating) and aim for a continuous, streamlined process. As a general guideline, fewer production steps are the key for low-cost sensors. Prioritizing simplicity in the overall product design—devices should be user-friendly, effective, and affordable.

Researchers are encouraged to provide detailed cost analyses of electrode materials and production expenses in their sensor publications. For instance, Perju et al. demonstrated a comprehensive breakdown of material costs for their electrode manufacturing [83]. Additionally, consider estimating the energy consumption associated with power-intensive steps (e.g., using ovens, heat plates, laser scribing, or electrospinning) in kilowatt-hours (kWh). This holistic approach ensures transparency and facilitates informed decision-making.

6.7. Practical considerations

Numerous studies investigating new electrode materials utilize chronoamperometry in stirred solutions. However, it is crucial to assess whether this approach aligns with the final intended application. The primary benefit of employing a stirred solution lies in the increase mass transport through convection and the ability to conduct chronoamperometry until the signal stabilizes. This stabilization leads to improved standard deviation of the blank due to reduced signal fluctuations, resulting in significantly enhanced limits of detection (LODs). Additionally, the stirred approach permits the homogenous incremental addition of the analyte, facilitating the construction of a calibration curve using the same electrode within a single measurement. Furthermore, using a stirred measurement approach enhances mass transport, and since we patiently await a stable signal, there are no abrupt charging currents or background current shifts, as seen in non-stirred approaches when initiating a new measurement for each analyte concentration. Therefore, extremely low LODs have been achieved when performed the measurement using stirred approach.

Although the stirred approach may be practical in clinical settings or well-equipped laboratories, it is considered impractical for POC testing because users typically prefer a simpler method: directly adding the sample onto the electrode and initiating the measurement. Despite its convenience for users, the non-stirred approach presents challenges. It exhibits charging current at the measurement's outset, and variations in background currents occur from electrode to electrode and measurement to measurement, ultimately leading to poorer LODs. As a result,

enhancing the detection sensitivity and tackling the challenges of non-stirred approaches is encouraged. Hereby, alternative strategies are required to address the unique challenges associated with this approach. For example, in our research group, we developed a non-stirred hydrogen peroxide sensor. Here, as part of the pretreatment, we needed to perform ten consecutive measurements in the blank at the same potential as the measurement itself, in order to ensure a stable background current before introducing hydrogen peroxide [79]. If the resulting LODs of the non-stirred approach are not low enough for the desired application, an implementation of user-friendly and simple strategies to preconcentrate or purify the samples before measurement could be used [136].

Another practical consideration for researchers is that some enzyme-free sensors face challenges in oxygen-dissolved solutions, as the presence of dissolved oxygen can interfere with the sensor's performance [193]. This problem is often addressed by attempting to remove oxygen by bubbling nitrogen (N_2) through the solution, which is highly impractical for real applications. To address this issue, one potential solution is to incorporate oxygen-scavenging molecules into the sample such as sodium thiosulfate or ascorbic acid, which can remove or neutralize dissolved oxygen. However, these oxygen-scavengers could lead to interfering signals at the electrode (due to the low oxidation potential) or quench analytes such as hydrogen peroxide which need to be critically investigated [193]. Additionally, electrochemical filters can be used to remove oxygen [194]. In this method, a porous electrode is placed on top of the electrochemical sensor, separated by an additional porous layer, allowing for the electrochemically induced oxygen-reduction reaction to remove oxygen. However, it is important to consider that the electrochemical removal of oxygen may change the local pH near the electrochemical sensor. Another approach could involve the development of sensor materials that are inherently resistant to oxygen interference, ensuring reliable performance even in oxygen-rich environments.

7. Conclusion and outlook

The review provides an overview of the advancement in non-enzymatic sensors and their potential applications towards point-of-care (POC) testing. Various strategies including conventional techniques, e.g., screen printing, and emerging strategy, have been employed for generating non-enzymatic electrodes in a mass-producing manner which will ultimately provide POC devices with low cost. In this regard, we, however, evaluate the pros and cons of each technique. Moreover, we also provide characteristics of sample matrices as well as relevant analytes which need to be considered to efficiently apply non-enzymatic sensors, raising specific points of concern in sensor development. In addition, the poorer selectivity of non-enzymatic sensors in comparison to enzymatic counterparts is still very challenging. With this, molecular imprinting technology has become a promising solution which is also discussed in this review. We lastly give the discussion on other remaining challenges and some published studies as well as our viewpoints, which are promising to tackle such issues. In addition to this, we also want to give our perspective in the light of fabrication to end-users which could make non-enzymatic sensors to be more attractive for POC testing.

Although various kinds of fabrication technology have been proposed for generating non-enzymatic transducers, only some of them possess potential for POC devices considering speed and cost of production. Herein, screen-printing and roll-to-roll (R2R) printing are well-established techniques, allowing massive production of electrodes within a short time period. However, manufacturers must critically investigate the catalyst-ink formulation to ensure its homogeneity and consequently electrode reproducibility. Typically, catalysts need to be blended with other conductive materials, e.g. carbon powder, and binding agent to assist printing and film formation process. This makes the embedded catalyst not useful, raising the concern about their cost-

effectiveness, in particular, with costly catalyst materials. Therefore, creating a very thin film or developing the printing of pure catalysts would be favorable. In addition, further studies on adhesion between the formulated ink and various substrates, e.g., paper and textile materials, would allow the applications of non-enzymatic sensors to be expandable.

Apart from the conventional strategies, laser-induced carbon-graphene hybrid technology has emerged and gained popularity nowadays. Unlike thin film electrodes obtained from screen-printing and R2R printing, the laser-based fabrication method provides 3D-porous film with immense surface area which can rationally boost detection sensitivity. Even though the initial investment cost is high, it is considered effective for the long run overall. Nevertheless, laser-scribing technology is at an early stage which requires more development and careful attention. For example, highly porous electrodes, on the one hand, are highly sensitive but could potentially, on the other hand, cause poor reproducibility of the signal as well. This is because rough surfaces with microstructure typically exhibit hydrophobic properties which hinder inhomogeneous contact between aqueous solutions and electrodes. Thus, high wettability of the entire electrode surface must be ensured. This could be probably done by plasma treatment or chemical treatment. However, in case the problem still exists, variation between electrode-to-electrode may be solved by ratio metric measurements in which internal reference signal is used for signal normalization. Furthermore, properties of laser-induced non-enzymatic electrodes after production must be carefully investigated. Based on our experience, the freshly produced electrodes yield high sensitivity, but the performance diminished over time after storage. Studies on storage conditions or development of protective coatings are encouraged to standardize electrode's property.

Various sample matrices constitute not only different levels of analyte but also distinct potential interferences which pose significant challenges in non-enzymatic sensors. Although blood contains a high abundance of analyte and is widely used in clinical diagnostics, other biological fluids which can be accessed non-invasively and contain fewer interfering species are preferential. These fluids include sweat, saliva, urine, and breath. However, the analytes in such biological samples are typically in a low amount. Therefore, highly sensitive non-enzymatic sensors are majorly required. Concerning the lag time, comparison analyte levels between blood and non-invasive biological fluids must be intensively conducted to guarantee reliability of the result. In addition to clinical samples, non-enzymatic sensors possess potential applications in measurement of analyte in water, food and beverages, and cell culture medium in bioprocess. Except water, the non-clinical samples typically contain high amount of analytes and interfering species. Most of reports suppress the interfering effect by diluting samples with measurement buffer. Nevertheless, an extreme dilution could potentially cause errors as analyte concentrations are reduced as well.

Selectivity towards analyte of interest is one of a major concern in the field of non-enzymatic sensors. Molecular imprinting technology is a highly promising strategy to tackle this issue. Some studies have successfully shown that molecular imprinted polymer on non-enzymatic sensor surface can assist the selective binding of interested analyte which can be subsequently catalyzed by the catalyst. In addition to enabling selective binding, molecular imprinting polymer is considered helpful as a protecting layer which may further prevent biofouling and other interfering electroactive species to contact the catalyst. In our opinion, there have been many rooms for further investigations regarding non-enzymatic sensors coating with molecular imprinting polymer.

Finally, as discussed in the remaining challenges there have been many promising studies which can be exploited to over the issues. With these altogether and further developments we strongly believe that non-enzymatic sensors will eventually become a robust and viable tool in POC testing in the future where desired analytical performance can be achieved in an affordable manner which eventually can improve quality

of life.

CRediT authorship contribution statement

Christoph Bruckschlegel: Writing – review & editing, Writing – original draft, Visualization, Validation. **Vivien Fleischmann:** Writing – review & editing, Writing – original draft. **Nenad Gajovic-Eichelmann:** Writing – review & editing, Writing – original draft, Conceptualization. **Nongnoot Wongkaew:** Writing – review & editing, Writing – original draft, Project administration, Funding acquisition, Conceptualization.

Declaration of competing interest

The authors declare that they have no known competing financial interests or personal relationships that could have appeared to influence the work reported in this paper.

Acknowledgment

This work received research grants from Deutsche Forschungsgemeinschaft (project no. 457100614).

Data availability

No data was used for the research described in the article.

References

- [1] S. Wild, G. Roglic, A. Green, R. Sicree, H. King, Global prevalence of diabetes: estimates for the year 2000 and projections for 2030, *Diabetes Care* 27 (2004) 1047–1053, <https://doi.org/10.2337/diacare.27.5.1047>.
- [2] International Diabetes Federation, Facts & figures (<https://idf.org/about-diabetes/diabetes-facts-figures/>).
- [3] Grand View Research, Point of care diagnostics market size, share & trends analysis report by product (infectious diseases, glucose testing, Cardiac Markers), by End-Use (Clinics, Home, Hospitals), by Region, and Segment Forecasts, 2024 - 2030.
- [4] E.T.S.G. da Silva, D.E.P. Souto, J.T.C. Barragan, J. de F. Giarola, A.C.M. de Moraes, L.T. Kubota, Electrochemical biosensors in point-of-care devices: recent advances and future trends, *Chemelectrochem* 4 (2017) 778–794, <https://doi.org/10.1002/celc.201600758>.
- [5] Y. Liu, X. Luo, Q. Yu, Le Ye, L. Yang, Y. Cui, Review of point-of-care platforms for diabetes: (1) sensing, *Sensors and Actuators Reports* 4 (2022) 100113, <https://doi.org/10.1016/j.snr.2022.100113>.
- [6] K.E. Toghill, R.G. Compton, Electrochemical non-enzymatic glucose sensors: a perspective and an evaluation, *Int. J. Electrochem. Sci.* 5 (2010) 1246–1301, [https://doi.org/10.1016/S1452-3981\(23\)15359-4](https://doi.org/10.1016/S1452-3981(23)15359-4).
- [7] W. He, Y. Huang, J. Wu, Enzyme-free glucose biosensors based on MoS₂ nanocomposites, *Nanoscale Res. Lett.* 15 (2020) 60, <https://doi.org/10.1186/s11671-020-3285-3>.
- [8] L.-M. Lu, H.-B. Li, F. Qu, X.-B. Zhang, G.-L. Shen, R.-Q. Yu, In situ synthesis of palladium nanoparticle-graphene nanohybrids and their application in nonenzymatic glucose biosensors, *Biosens. Bioelectron.* 26 (2011) 3500–3504, <https://doi.org/10.1016/j.bios.2011.01.033>.
- [9] Y. Zhang, X. Xiao, Y. Sun, Y. Shi, H. Dai, P. Ni, J. Hu, Z. Li, Y. Song, L. Wang, Electrochemical deposition of nickel nanoparticles on reduced graphene oxide film for nonenzymatic glucose sensing, *Electroanalysis* 25 (2013) 959–966, <https://doi.org/10.1002/elan.201200479>.
- [10] N.M. Kilic, S. Singh, G. Keles, S. Cinti, S. Kurbanoglu, D. Odaci, Novel approaches to enzyme-based electrochemical nanobiosensors, *Biosensors* 13 (2023), <https://doi.org/10.3390/bios1306022>.
- [11] A. Raziq, M. Tariq, R. Hussian, M.H. Mehmood, M.S. Khan, A. Hassan, Electrochemical investigation of glucose oxidation on a glassy carbon electrode using voltammetric, amperometric, and digital simulation methods, *ChemistrySelect* 2 (2017) 9711–9717, <https://doi.org/10.1002/slct.201701193>.
- [12] P. Si, Y. Huang, T. Wang, J. Ma, Nanomaterials for electrochemical non-enzymatic glucose biosensors, *RSC Adv.* 3 (2013) 3487, <https://doi.org/10.1039/C2RA22360K>.
- [13] C. Zhou, J. Feng, Y. Tian, Y. Wu, Q. He, G. Li, J. Liu, Non-enzymatic electrochemical sensors based on nanomaterials for detection of organophosphorus pesticide residues, *Environ. Sci.: Adv.* 2 (2023) 933–956, <https://doi.org/10.1039/D3VA00045A>.
- [14] D. Thatikayala, D. Ponnammam, K.K. Sadasivuni, J.-J. Cabibihan, A.K. Al-Ali, R. A. Malik, B. Min, Progress of advanced nanomaterials in the non-enzymatic electrochemical sensing of glucose and H₂O₂, *Biosensors* 10 (2020), <https://doi.org/10.3390/bios10110151>.
- [15] Y. Liu, T. Liu, D. Jiang, Non-enzymatic electrochemical sensor for wearable monitoring of sweat biomarkers: a mini-review, *Current Research in Biotechnology* 6 (2023) 100143, <https://doi.org/10.1016/j.crbiot.2023.100143>.
- [16] M.H. Hassan, C. Vyas, B. Grieve, P. Bartolo, Recent advances in enzymatic and non-enzymatic electrochemical glucose sensing, *Sensors (Basel, Switzerland)* 21 (2021), <https://doi.org/10.3390/s21144672>.
- [17] M. Simsek, N. Wongkaew, Carbon nanomaterial hybrids via laser writing for high-performance non-enzymatic electrochemical sensors: a critical review, *Anal. Bioanal. Chem.* 413 (2021) 6079–6099, <https://doi.org/10.1007/s00216-021-03382-9>.
- [18] A.J. González Fà, V. Orazi, E.A. González, A. Juan, I. López-Corral, DFT study of β-d-glucose adsorption on single-walled carbon nanotubes decorated with platinum. A bonding analysis, *Appl. Surf. Sci.* 423 (2017) 542–548, <https://doi.org/10.1016/j.apsusc.2017.05.227>.
- [19] S.-S. Wang, W.-J. Qiu, T.-P. Wang, C.-L. Lee, Tuning structures of Pt shells on Pd nanocubes as neutral glucose oxidation catalysts and sensors, *Appl. Surf. Sci.* 605 (2022) 154670, <https://doi.org/10.1016/j.apsusc.2022.154670>.
- [20] Y. Shi, Z.-R. Ma, Y.-Y. Xiao, Y.-C. Yin, W.-M. Huang, Z.-C. Huang, Y.-Z. Zheng, F.-Y. Mu, R. Huang, G.-Y. Shi, Y.-Y. Sun, X.-H. Xia, W. Chen, Electronic metal-support interaction modulates single-atom platinum catalysis for hydrogen evolution reaction, *Nat. Commun.* 12 (2021) 3021, <https://doi.org/10.1038/s41467-021-23306-6>.
- [21] S. Park, S. Park, R.-A. Jeong, H. Boo, J. Park, H.C. Kim, T.D. Chung, Nonenzymatic continuous glucose monitoring in human whole blood using electrified nanoporous Pt, *Biosens. Bioelectron.* 31 (2012) 284–291, <https://doi.org/10.1016/j.bios.2011.10.033>.
- [22] T.-M. Cheng, T.-K. Huang, H.-K. Lin, S.-P. Tung, Y.-L. Chen, C.-Y. Lee, H.-T. Chiu, (110)-exposed gold nanocoral electrode as low onset potential selective glucose sensor, *ACS Appl. Mater. Interfaces* 2 (2010) 2773–2780, <https://doi.org/10.1021/am100432a>.
- [23] X. Niu, M. Lan, H. Zhao, C. Chen, Highly sensitive and selective nonenzymatic detection of glucose using three-dimensional porous nickel nanostructures, *Anal. Chem.* 85 (2013) 3561–3569, <https://doi.org/10.1021/ac3030976>.
- [24] X. Liu, W. Yang, L. Chen, J. Jia, Three-dimensional copper foam supported CuO nanowire arrays: an efficient non-enzymatic glucose sensor, *Electrochim. Acta* 235 (2017) 519–526, <https://doi.org/10.1016/j.electacta.2017.03.150>.
- [25] L. Kang, D. He, L. Bie, P. Jiang, Nanoporous cobalt oxide nanowires for non-enzymatic electrochemical glucose detection, *Sensor. Actuator. B Chem.* 220 (2015) 888–894, <https://doi.org/10.1016/j.snb.2015.06.015>.
- [26] S. Nantaphol, T. Watanabe, N. Nomura, W. Siangproh, O. Chailapakul, Y. Einaga, Bimetallic Pt-Au nanocatalysts electrochemically deposited on boron-doped diamond electrodes for nonenzymatic glucose detection, *Biosens. Bioelectron.* 98 (2017) 76–82, <https://doi.org/10.1016/j.bios.2017.06.034>.
- [27] H. Mei, H. Wu, W. Wu, S. Wang, Q. Xia, Ultrasensitive electrochemical assay of hydrogen peroxide and glucose based on PtNi alloy decorated MWCNTs, *RSC Adv.* 5 (2015) 102877–102884, <https://doi.org/10.1039/C5RA17410D>.
- [28] M. Abbasnia Tehrani, S.H. Ahmadi, S. Alimohammadi, P. Sasanpour, N. Batvani, S.H. Kazemi, M.A. Kiani, Continuous glucose monitoring using wearable non-enzymatic sensors in a physiological environment, *Biosens. Bioelectron.* X 18 (2024) 100482, <https://doi.org/10.1016/j.biosx.2024.100482>.
- [29] S.S. Nemati, G. Dehghan, S. Rastbary, T.N. Tan, A. Khataee, Enzyme-based and enzyme-free metal-based glucose biosensors: classification and recent advances, *Microchem. J.* 193 (2023) 109038, <https://doi.org/10.1016/j.microc.2023.109038>.
- [30] W.-C. Lee, K.-B. Kim, N.G. Gurudatt, K.K. Hussain, C.S. Choi, D.-S. Park, Y.-B. Shim, Comparison of enzymatic and non-enzymatic glucose sensors based on hierarchical Au-Ni alloy with conductive polymer, *Biosens. Bioelectron.* 130 (2019) 48–54, <https://doi.org/10.1016/j.bios.2019.01.028>.
- [31] A. Kaliyaraj Selva Kumar, Y. Zhang, D. Li, R.G. Compton, A mini-review: how reliable is the drop casting technique? *Electrochem. Commun.* 121 (2020) 106867, <https://doi.org/10.1016/j.elecom.2020.106867>.
- [32] X. Yu, R. Xing, Z. Peng, Y. Lin, Z. Du, J. Ding, L. Wang, Y. Han, To inhibit coffee ring effect in inkjet printing of light-emitting polymer films by decreasing capillary force, *Chin. Chem. Lett.* 30 (2019) 135–138, <https://doi.org/10.1016/j.ccllet.2018.09.007>.
- [33] Inkjet Printing of Well-Defined Polymer Dots and Arrays.
- [34] H.-Y. Ko, J. Park, H. Shin, J. Moon, Rapid self-assembly of monodisperse colloidal spheres in an ink-jet printed droplet, *Chem. Mater.* 16 (2004) 4212–4215, <https://doi.org/10.1021/cm035256t>.
- [35] H.B. Eral, D.M. Augustine, M.H.G. Duits, F. Mugele, Suppressing the coffee stain effect: how to control colloidal self-assembly in evaporating drops using electrowetting, *Soft Matter* 7 (2011) 4954, <https://doi.org/10.1039/C1SM05183K>.
- [36] P.-J. Yunker, T. Still, M.A. Lohr, A.G. Yodh, Suppression of the coffee-ring effect by shape-dependent capillary interactions, *Nature* 476 (2011) 308–311, <https://doi.org/10.1038/nature10344>.
- [37] D. Mampallil, J. Reboud, R. Wilson, D. Wylie, D.R. Klug, J.M. Cooper, Acoustic suppression of the coffee-ring effect, *Soft Matter* 11 (2015) 7207–7213, <https://doi.org/10.1039/C5SM01196E>.
- [38] H. Hu, R.G. Larson, Marangoni effect reverses coffee-ring depositions, *J. Phys. Chem. B* 110 (2006) 7090–7094, <https://doi.org/10.1021/jp0609232>.
- [39] H. Kawakami, Y. Ito, Y.-A. Chien, C.-Y. Chen, W.-T. Chiu, P. Chakraborty, T. Nakamoto, M. Sone, T.-F.M. Chang, Development of polypyrrole/nano-gold composite for non-enzymatic glucose sensors, *Micro and Nano Engineering* 14 (2022) 100109, <https://doi.org/10.1016/j.mne.2022.100109>.

- [40] H. Shu, L. Cao, G. Chang, H. He, Y. Zhang, Y. He, Direct electrodeposition of gold nanostructures onto glassy carbon electrodes for non-enzymatic detection of glucose, *Electrochim. Acta* 132 (2014) 524–532, <https://doi.org/10.1016/j.electacta.2014.04.031>.
- [41] P. Viswanathan, J.W. Kim, S. Manivannan, K. Kim, Methionine-assisted electrodeposition of porous copper cobalt bi-metallic hetero-nanostructures on an indium tin oxide electrode: a disposable and stable electrode for non-enzymatic glucose sensing, *J. Mater. Chem. C* 12 (2024) 7673–7683, <https://doi.org/10.1039/d4tc00079j>.
- [42] M. Simsek, K. Hoecherl, M. Schlosser, A.J. Baeumner, N. Wongkaew, Printable 3D carbon nanofiber networks with embedded metal nanocatalysts, *ACS Appl. Mater. Interfaces* 12 (2020) 39533–39540, <https://doi.org/10.1021/acsami.0c08926>.
- [43] R.R. Suresh, M. Lakshmanakumar, J.B.B. Arockia Jayalatha, K.S. Rajan, S. Sethuraman, U.M. Krishnan, J.B.B. Rayappan, Fabrication of screen-printed electrodes: opportunities and challenges, *J. Mater. Sci.* 56 (2021) 8951–9006, <https://doi.org/10.1007/s10853-020-05499-1>.
- [44] W.-Y. Su, S.-M. Wang, S.-H. Cheng, Electrochemically pretreated screen-printed carbon electrodes for the simultaneous determination of aminophenol isomers, *J. Electroanal. Chem.* 651 (2011) 166–172, <https://doi.org/10.1016/j.jelechem.2010.11.028>.
- [45] D. Antuña-Jiménez, M.B. González-García, D. Hernández-Santos, P. Fanjul-Bolado, Screen-printed electrodes modified with metal nanoparticles for small molecule sensing, *Biosensors* 10 (2020), <https://doi.org/10.3390/bios10020009>.
- [46] Z. Chu, J. Peng, W. Jin, Advanced nanomaterial inks for screen-printed chemical sensors, *Sensor. Actuator. B Chem.* 243 (2017) 919–926, <https://doi.org/10.1016/j.snb.2016.12.022>.
- [47] W. Yin, D.-H. Lee, J. Choi, C. Park, S.M. Cho, Screen printing of silver nanoparticle suspension for metal interconnects, *Kor. J. Chem. Eng.* 25 (2008) 1358–1361, <https://doi.org/10.1007/s11814-008-0223-y>.
- [48] S. Abdolhosseinzadeh, R. Schneider, A. Verma, J. Heier, F. Nüesch, C.J. Zhang, Turning trash into treasure: additive free MXene sediment inks for screen-printed micro-supercapacitors, *Advanced materials* (Deerfield Beach, Fla.) 32 (2020) e2000716, <https://doi.org/10.1002/adma.202000716>.
- [49] A. Romeo, A. Moya, T.S. Leung, G. Gabriel, R. Villa, S. Sánchez, Inkjet printed flexible non-enzymatic glucose sensor for tear fluid analysis, *Appl. Mater. Today* 10 (2018) 133–141, <https://doi.org/10.1016/j.apmt.2017.12.016>.
- [50] P. Sundriyal, S. Bhattacharya, Inkjet-printed electrodes on A4 paper substrates for low-cost, disposable, and flexible asymmetric supercapacitors, *ACS Appl. Mater. Interfaces* 9 (2017) 38507–38521, <https://doi.org/10.1021/acsami.7b11262>.
- [51] A. Hussain, N. Abbas, A. Ali, Inkjet printing: a viable technology for biosensor fabrication, *Chemosensors* 10 (2022) 103, <https://doi.org/10.3390/chemosensors10030103>.
- [52] Y. Ooi, I. Hanasaki, D. Mizumura, Y. Matsuda, Suppressing the coffee-ring effect of colloidal droplets by dispersed cellulose nanofibers, *Sci. Technol. Adv. Mater.* 18 (2017) 316–324, <https://doi.org/10.1080/14686996.2017.1314776>.
- [53] B. Zhao, M. Lu, Z. Wang, Z. Jiao, P. Hu, Q. Gao, Y. Jiang, L. Cheng, Self-assembly of ultrathin MnO₂/graphene with three-dimension hierarchical structure by ultrasonic-assisted co-precipitation method, *J. Alloys Compd.* 663 (2016) 180–186, <https://doi.org/10.1016/j.jallcom.2015.12.018>.
- [54] H. Shamkhalichenar, J.-W. Choi, An inkjet-printed non-enzymatic hydrogen peroxide sensor on paper, *J. Electrochem. Soc.* 164 (2017) B3101–B3106, <https://doi.org/10.1149/2.0161705jes>.
- [55] R. Ahmad, M. Vaseem, N. Tripathy, Y.-B. Hahn, Wide linear-range detecting nonenzymatic glucose biosensor based on CuO nanoparticles inkjet-printed on electrodes, *Anal. Chem.* 85 (2013) 10448–10454, <https://doi.org/10.1021/ac402925r>.
- [56] S. Uzun, M. Schelling, K. Hantanasirisakul, T.S. Mathis, R. Askeland, G. Dion, Y. Gogotsi, Additive-free aqueous MXene inks for thermal inkjet printing on textiles, *Small* 17 (2021), <https://doi.org/10.1002/sml.202006376>.
- [57] L.A. Pradela-Filho, D.A.G. Araújo, V.N. Ataíde, G.N. Meloni, T.R.L.C. Paixão, Challenges faced with 3D-printed electrochemical sensors in analytical applications, *Anal. Bioanal. Chem.* 416 (2024) 4679–4690, <https://doi.org/10.1007/s00216-024-05308-7>.
- [58] R.G. Rocha, R.M. Cardoso, P.J. Zambiasi, S.V.F. Castro, T.V.B. Ferraz, G.d. O. Aparecido, J.A. Bonacin, R.A.A. Munoz, E.M. Richter, Production of 3D-printed disposable electrochemical sensors for glucose detection using a conductive filament modified with nickel microparticles, *Anal. Chim. Acta* 1132 (2020) 1–9, <https://doi.org/10.1016/j.aca.2020.07.028>.
- [59] M. Bariya, Z. Shahpar, H. Park, J. Sun, Y. Jung, W. Gao, H.Y.Y. Nyein, T.S. Liaw, L.-C. Tai, Q.P. Ngo, M. Chao, Y. Zhao, M. Hettick, G. Cho, A. Javey, Roll-to-roll gravure printed electrochemical sensors for wearable and medical devices, *ACS Nano* 12 (2018) 6978–6987, <https://doi.org/10.1021/acs.nano.8b02505>.
- [60] G.R. Cagnani, G. Ibáñez-Redín, B. Tirich, D. Gonçalves, D.T. Balogh, O. N. Oliveira, Fully-printed electrochemical sensors made with flexible screen-printed electrodes modified by roll-to-roll slot-die coating, *Biosens. Bioelectron.* 165 (2020) 112428, <https://doi.org/10.1016/j.bios.2020.112428>.
- [61] G. Ibáñez-Redín, G. Rosso Cagnani, N. O. Gomes, P.A. Raymundo-Pereira, S.A. S. Machado, M.A. Gutierrez, J.E. Krieger, O.N. Oliveira, Wearable potentiometric biosensor for analysis of urea in sweat, *Biosens. Bioelectron.* 223 (2023) 114994, <https://doi.org/10.1016/j.bios.2022.114994>.
- [62] K. Chawang, S. Bing, J.-C. Chiao, Printable and flexible iridium oxide-based pH sensor by a roll-to-roll process, *Chemosensors* 11 (2023) 267, <https://doi.org/10.3390/chemosensors11050267>.
- [63] C.M. Fung, J.S. Lloyd, S. Samavat, D. Deganello, K.S. Teng, Facile fabrication of electrochemical ZnO nanowire glucose biosensor using roll to roll printing technique, *Sensor. Actuator. B Chem.* 247 (2017) 807–813, <https://doi.org/10.1016/j.snb.2017.03.105>.
- [64] R. Ye, Z. Peng, T. Wang, Y. Xu, J. Zhang, Y. Li, L.G. Niewski, J. Lin, J.M. Tour, In situ formation of metal oxide nanocrystals embedded in laser-induced graphene, *ACS Nano* 9 (2015) 9244–9251, <https://doi.org/10.1021/acs.nano.5b04138>.
- [65] L. Fan, R. Wu, V. Patel, J.J. Huang, P.R. Selvaganapathy, Solid-state, reagent-free and one-step laser-induced synthesis of graphene-supported metal nanocomposites from metal leaves and application to glucose sensing, *Anal. Chim. Acta* 1264 (2023) 341248, <https://doi.org/10.1016/j.aca.2023.341248>.
- [66] Y. Zhang, C. Zhang, W. Chen, Z. Liu, One-step laser-induced Cu-embedded graphene for non-enzymatic glucose sensing in beverages, *J. Alloys Compd.* 992 (2024) 174563, <https://doi.org/10.1016/j.jallcom.2024.174563>.
- [67] J. Zhao, C. Zheng, J. Gao, J. Gui, L. Deng, Y. Wang, R. Xu, Co3O4 nanoparticles embedded in laser-induced graphene for a flexible and highly sensitive enzyme-free glucose biosensor, *Sensor. Actuator. B Chem.* 347 (2021) 130653, <https://doi.org/10.1016/j.snb.2021.130653>.
- [68] A. Scroccarello, R. Álvarez-Dídez, F. Della Pelle, C. de Carvalho Castro E Silva, A. Idili, C. Parolo, D. Compagnone, A. Merkoçi, One-step laser nanostructuring of reduced graphene oxide films embedding metal nanoparticles for sensing applications, *ACS Sens.* 8 (2023) 598–609, <https://doi.org/10.1021/acssensors.2c01782>.
- [69] Leanne Riley, Mean fasting blood glucose (<https://www.who.int/data/gho/indicator-metadata-registry/imr-details/2380>).
- [70] B.A. Patel, *Electrochemistry for Bioanalysis*, Elsevier, San Diego, 2021.
- [71] E.M. Mackay, L.L. Mackay, The concentration of urea in the blood of normal individuals, *JCI (J. Clin. Investig.)* 4 (1927) 295–306, <https://doi.org/10.1172/JCI100124>.
- [72] M. Labib, E.H. Sargent, S.O. Kelley, Electrochemical methods for the analysis of clinically relevant biomolecules, *Chem. Rev.* 116 (2016) 9001–9090, <https://doi.org/10.1021/acs.chemrev.6b00220>.
- [73] Y. Ma, C. Ma, Y. Wang, K. Wang, Advanced nickel-based catalysts for urea oxidation reaction: challenges and developments, *Catalysts* 12 (2022) 337, <https://doi.org/10.3390/catal12030337>.
- [74] S. Kim, K. Kim, H.-J. Kim, H.-N. Lee, T.J. Park, Y.M. Park, Non-enzymatic electrochemical lactate sensing by NiO and Ni(OH)₂ electrodes: a mechanistic investigation, *Electrochim. Acta* 276 (2018) 240–246, <https://doi.org/10.1016/j.electacta.2018.04.172>.
- [75] R.J. Glynn, E.W. Campion, J.E. Silbert, Trends in serum uric acid levels 1961–1980, *Arthritis Rheum.* 26 (1983) 87–93, <https://doi.org/10.1002/art.1780260115>.
- [76] A.M. Butler, M. Cushman, Distribution of ascorbic acid in the blood and its nutritional significance, *JCI (J. Clin. Investig.)* 19 (1940) 459–467, <https://doi.org/10.1172/JCI101147>.
- [77] M. Lindblad, P. Tveden-Nyborg, J. Lykkesfeldt, Regulation of vitamin C homeostasis during deficiency, *Nutrients* 5 (2013) 2860–2879, <https://doi.org/10.3390/nu5082860>.
- [78] J.P. Moran, L. Cohen, J.M. Greene, G. Xu, E.B. Feldman, C.G. Hames, D. S. Feldman, Plasma ascorbic acid concentrations relate inversely to blood pressure in human subjects, *Am. J. Clin. Nutr.* 57 (1993) 213–217, <https://doi.org/10.1093/ajcn/57.2.213>.
- [79] C. Bruckschlegel, M. Schlosser, N. Wongkaew, Investigating nanocatalyst-embedding laser-induced carbon nanofibers for non-enzymatic electrochemical sensing of hydrogen peroxide, *Anal. Bioanal. Chem.* 415 (2023) 4487–4499, <https://doi.org/10.1007/s00216-023-04640-8>.
- [80] M. Seki, Biological significance and development of practical synthesis of biotin, *Med. Res. Rev.* 26 (2006) 434–482, <https://doi.org/10.1002/med.20058>.
- [81] S.J. Weinstein, T.J. Hartman, R. Stolzenberg-Solomon, P. Pietinen, M.J. Barrett, P.R. Taylor, J. Virtamo, D. Albanes, Null association between prostate cancer and serum folate, vitamin B₆, vitamin B₁₂, Homocysteine (2003) 1271–1272.
- [82] S.B. Revin, S.A. John, Simultaneous determination of vitamins B₂, B₉ and C using a heterocyclic conducting polymer modified electrode, *Electrochim. Acta* 75 (2012) 35–41, <https://doi.org/10.1016/j.electacta.2012.04.056>.
- [83] A. Perju, A.J. Baeumner, N. Wongkaew, Freestanding 3D-interconnected carbon nanofibers as high-performance transducers in miniaturized electrochemical sensors, *Mikrochim. Acta* 189 (2022) 424, <https://doi.org/10.1007/s00604-022-05492-2>.
- [84] E. Baldrich, F.X. Muñoz, Carbon nanotube wiring: a tool for straightforward electrochemical biosensing at magnetic particles, *Anal. Chem.* 83 (2011) 9244–9250, <https://doi.org/10.1021/ac201137q>.
- [85] S. Lin, C.-C. Liu, T.-C. Chou, Amperometric acetylcholine sensor catalyzed by nickel anode electrode, *Biosens. Bioelectron.* 20 (2004) 9–14, <https://doi.org/10.1016/j.bios.2004.01.018>.
- [86] R.T. Peaston, C. Weinkove, Measurement of catecholamines and their metabolites, *Ann. Clin. Biochem.* 41 (2004) 17–38, <https://doi.org/10.1258/000456304322664663>.
- [87] J. Eidenschink, S. Bagherimetkazini, F.-M. Matysik, Investigation of the electrochemical behavior of cysteine by hyphenation of electrochemistry and mass spectrometry, *Monatsh. Chem.* 153 (2022) 775–780, <https://doi.org/10.1007/s00706-022-02943-7>.
- [88] R.H. McMenamy, C.C. Lund, J.L. Oncley, Unbound amino acid concentrations in human blood plasmas, *JCI (J. Clin. Investig.)* 36 (1957) 1672–1679, <https://doi.org/10.1172/JCI103568>.
- [89] L. Calabresi, M. Gomaraschi, S. Simonelli, F. Bernini, G. Franceschini, HDL and atherosclerosis: insights from inherited HDL disorders, *Biochim. Biophys. Acta* 1851 (2015) 13–18, <https://doi.org/10.1016/j.bbalip.2014.07.015>.

- [90] J. Heikenfeld, A. Jajack, B. Feldman, S.W. Granger, S. Gaitonde, G. Begtrup, B. A. Katchman, Accessing analytes in biofluids for peripheral biochemical monitoring, *Nat. Biotechnol.* 37 (2019) 407–419, <https://doi.org/10.1038/s41587-019-0040-3>.
- [91] C. Scuffi, Interstitium versus blood equilibrium in glucose concentration and its impact on subcutaneous continuous glucose monitoring systems, *Eur. Endocrinol.* 10 (2014) 36–42, <https://doi.org/10.17925/EE.2014.10.01.36>.
- [92] J. Madden, C. O'Mahony, M. Thompson, A. O'Riordan, P. Galvin, Biosensing in dermal interstitial fluid using microneedle based electrochemical devices, *Sensing and Bio-Sensing Research* 29 (2020) 100348, <https://doi.org/10.1016/j.sbsr.2020.100348>.
- [93] M.J. Patterson, S.D. Galloway, M.A. Nimmo, Variations in regional sweat composition in normal human males, *Exp. Physiol.* 85 (2000) 869–875, <https://doi.org/10.1111/j.1469-445x.2000.02058.x>.
- [94] S. Robinson, A.H. Robinson, Chemical composition of sweat, *Physiol. Rev.* 34 (1954) 202–220, <https://doi.org/10.1152/physrev.1954.34.2.202>.
- [95] A. Hauke, P. Simmers, Y.R. Ojha, B.D. Cameron, R. Ballweg, T. Zhang, N. Twine, M. Brothers, E. Gomez, J. Heikenfeld, Complete validation of a continuous and blood-correlated sweat biosensing device with integrated sweat stimulation, *Lab Chip* 18 (2018) 3750–3759, <https://doi.org/10.1039/c8lc01082j>.
- [96] T.D. La Count, A. Jajack, J. Heikenfeld, G.B. Kasting, Modeling glucose transport from systemic circulation to sweat, *J. Pharmaceut. Sci.* 108 (2019) 364–371, <https://doi.org/10.1016/j.xphs.2018.09.026>.
- [97] J. Moyer, D. Wilson, I. Finkelshtein, B. Wong, R. Potts, Correlation between sweat glucose and blood glucose in subjects with diabetes, *Diabetes Technol. Therapeut.* 14 (2012) 398–402, <https://doi.org/10.1089/dia.2011.0262>.
- [98] H. Zafar, A. Channa, V. Jeoti, G.M. Stojanović, Comprehensive review on wearable sweat-glucose sensors for continuous glucose monitoring, *Sensors* (Basel, Switzerland) 22 (2022), <https://doi.org/10.3390/s22020638>.
- [99] H. Lee, Y.J. Hong, S. Baik, T. Hyeon, D.-H. Kim, Enzyme-based glucose sensor: from invasive to wearable device, *Adv. Healthcare Mater.* 7 (2018) e1701150, <https://doi.org/10.1002/adhm.201701150>.
- [100] L.B. Baker, A.S. Wolfe, Physiological mechanisms determining eccrine sweat composition, *Eur. J. Appl. Physiol.* 120 (2020) 719–752, <https://doi.org/10.1007/s00421-020-04323-7>.
- [101] L. Zhang, S. Xie, J. Gu, X. Wang, Fabrication of core-shell Pt-Ni(OH)₂ nanosheets on Ni foam and investigation on its detection performance of ammonia-nitrogen in lake and sea water, *J. Mater. Sci. Mater. Electron.* 34 (2023), <https://doi.org/10.1007/s10854-023-10386-x>.
- [102] C.T. Huang, M.L. Chen, L.L. Huang, I.F. Mao, Uric acid and urea in human sweat, *Chin. J. Physiol.* 45 (3) (2002) 109–116.
- [103] L. García-Carmona, A. Martín, J.R. Sempionatto, J.R. Moreto, M.C. González, J. Wang, A. Escarpa, Pacifier biosensor: toward noninvasive saliva biomarker monitoring, *Anal. Chem.* 91 (2019) 13883–13891, <https://doi.org/10.1021/acs.analchem.9b03379>.
- [104] T. Arakawa, Y. Kuroki, H. Nitta, P. Chouhan, K. Toma, S.-I. Sawada, S. Takeuchi, T. Sekita, K. Akiyoshi, S. Minakuchi, K. Mitsubayashi, Mouthguard biosensor with telemetry system for monitoring of saliva glucose: a novel cavitas sensor, *Biosens. Bioelectron.* 84 (2016) 106–111, <https://doi.org/10.1016/j.bios.2015.12.014>.
- [105] S. Gupta, M.T. Nayak, J.D. Sunitha, G. Dawar, N. Sinha, N.S. Rallan, Correlation of salivary glucose level with blood glucose level in diabetes mellitus, *Journal of oral and maxillofacial pathology JOMFP* 21 (2017) 334–339, <https://doi.org/10.4103/jomfp.JOMFP.222.15>.
- [106] M. Dhanya, S. Hegde, Salivary glucose as a diagnostic tool in Type II diabetes mellitus: a case-control study, *Niger. J. Clin. Pract.* 19 (2016) 486–490, <https://doi.org/10.4103/1119-3077.183314>.
- [107] W. Zhang, Y. Du, M.L. Wang, On-chip highly sensitive saliva glucose sensing using multilayer films composed of single-walled carbon nanotubes, gold nanoparticles, and glucose oxidase, *Sensing and Bio-Sensing Research* 4 (2015) 96–102, <https://doi.org/10.1016/j.sbsr.2015.04.006>.
- [108] A. Jaiswal, S. Madaan, N. Acharya, S. Kumar, D. Talwar, D. Dewani, Salivary uric acid: a noninvasive wonder for clinicians? *Cureus* 13 (2021) e19649 <https://doi.org/10.7759/cureus.19649>.
- [109] D.O. Temilola, K. Bezuidenhout, R.T. Erasmus, L. Stephen, M.R. Davids, H. Holmes, Salivary creatinine as a diagnostic tool for evaluating patients with chronic kidney disease, *BMC Nephrol.* 20 (2019) 387, <https://doi.org/10.1186/s12882-019-1546-0>.
- [110] K.S. Eom, Y.J. Lee, H.W. Seo, J.Y. Kang, J.S. Shim, S.H. Lee, Sensitive and non-invasive cholesterol determination in saliva via optimization of enzyme loading and platinum nano-cluster composition, *Analyst* 145 (2020) 908–916, <https://doi.org/10.1039/C9AN01679A>.
- [111] D.K. Shruthi, S.M. Channabasappa, K.M. Mithun, B.S. Suresh, A.S. Tegginamani, T. Smitha, The role of salivary lactate levels in assessing the severity of septic shock, *Journal of oral and maxillofacial pathology JOMFP* 25 (2021) 437–440, <https://doi.org/10.4103/jomfp.jomfp.199.21>.
- [112] A.G. Cardoso, H. Viltres, G.A. Ortega, V. Phung, R. Grewal, H. Mozaffari, S. R. Ahmed, A.R. Rajabzadeh, S. Srinivasan, Electrochemical sensing of analytes in saliva: challenges, progress, and perspectives, *TrAC, Trends Anal. Chem.* 160 (2023) 116965, <https://doi.org/10.1016/j.trac.2023.116965>.
- [113] O. Adeniyi, N. Nwahara, D. Mwanza, T. Nyokong, P. Mashazi, Nanohybrid electrocatalyst based on cobalt phthalocyanine-carbon nanotube-reduced graphene oxide for ultrasensitive detection of glucose in human saliva, *Sensor. Actuator. B Chem.* 348 (2021) 130723, <https://doi.org/10.1016/j.snb.2021.130723>.
- [114] X. Li, C. Zhan, Q. Huang, M. He, C. Yang, C. Yang, X. Huang, M. Chen, X. Xie, H.-J. Chen, Smart diaper based on integrated multiplex carbon nanotube-coated electrode array sensors for in situ urine monitoring, *ACS Appl. Nano Mater.* 5 (2022) 4767–4778, <https://doi.org/10.1021/acsnm.1c04220>.
- [115] N. Sarigul, F. Korkmaz, I. Kurultak, A new artificial urine protocol to better imitate human urine, *Sci. Rep.* 9 (2019) 20159, <https://doi.org/10.1038/s41598-019-56693-4>.
- [116] S. Das, M. Pal, Review—non-invasive monitoring of human health by exhaled breath analysis: a comprehensive review, *J. Electrochem. Soc.* 167 (2020) 37562, <https://doi.org/10.1149/1945-7111/ab76a6>.
- [117] D. Maier, E. Laubender, A. Basavanna, S. Schumann, F. Güder, G.A. Urban, C. Dincer, Toward continuous monitoring of breath biochemistry: a paper-based wearable sensor for real-time hydrogen peroxide measurement in simulated breath, *ACS Sens.* 4 (2019) 2945–2951, <https://doi.org/10.1021/acssensors.9b01403>.
- [118] D. Tankasala, J.C. Linnes, Noninvasive glucose detection in exhaled breath condensate, *Translational research the journal of laboratory and clinical medicine* 213 (2019) 1–22, <https://doi.org/10.1016/j.trsl.2019.05.006>.
- [119] Y. Sakumura, Y. Koyama, H. Tokutake, T. Hida, K. Sato, T. Itoh, T. Akamatsu, W. Shin, Diagnosis by volatile organic compounds in exhaled breath from lung cancer patients using support vector machine algorithm, *Sensors* (Basel, Switzerland) 17 (2017), <https://doi.org/10.3390/s17020287>.
- [120] K. Bloemen, G. Lissens, K. Desager, G. Schoeters, Determinants of variability of protein content, volume and pH of exhaled breath condensate, *Respir. Med.* 101 (2007) 1331–1337, <https://doi.org/10.1016/j.rmed.2006.10.008>.
- [121] S.A. Hayes, S. Haeffliger, B. Harris, N. Pavlakis, S.J. Clarke, M.P. Molloy, V. M. Howell, Exhaled breath condensate for lung cancer protein analysis: a review of methods and biomarkers, *J. Breath Res.* 10 (2016) 34001, <https://doi.org/10.1088/1752-7155/10/3/034001>.
- [122] European Environment Agency, *Industrial Pollutant Releases to Water in Europe, 2024*.
- [123] M.S. de Ilurdoz, J.J. Sadhwani, J.V. Reboso, Antibiotic removal processes from water & wastewater for the protection of the aquatic environment - a review, *J. Water Proc. Eng.* 45 (2022) 102474, <https://doi.org/10.1016/j.jwpe.2021.102474>.
- [124] V. Karthik, P. Selvakumar, P. Senthil Kumar, V. Satheeskumar, M. Godwin Vijaysunder, S. Hariharan, K. Antony, Recent advances in electrochemical sensor developments for detecting emerging pollutant in water environment, *Chemosphere* 304 (2022) 135331, <https://doi.org/10.1016/j.chemosphere.2022.135331>.
- [125] Y. Liu, Q. Xue, C. Chang, R. Wang, Z. Liu, L. He, Recent progress regarding electrochemical sensors for the detection of typical pollutants in water environments, *Analytical sciences the international journal of the Japan Society for Analytical Chemistry* 38 (2022) 55–70, <https://doi.org/10.2116/analsci.21SAR12>.
- [126] G. Cho, S. Azzouzi, G. Zucchi, B. Lebental, Electrical and electrochemical sensors based on carbon nanotubes for the monitoring of chemicals in water-A review, *Sensors* (Basel, Switzerland) 22 (2021), <https://doi.org/10.3390/s22010218>.
- [127] K.E. Goodman, T. Hua, Q.-X.A. Sang, Effects of polystyrene microplastics on human kidney and liver cell morphology, cellular proliferation, and metabolism, *ACS Omega* 7 (2022) 34136–34153, <https://doi.org/10.1021/acsomega.2c03453>.
- [128] M.F. Altahan, A.G. Ali, A.A. Hathoot, M.A. Azzem, Modified electrode decorated with silver as a novel non-enzymatic sensor for the determination of ammonium in water, *Sci. Rep.* 13 (2023) 16861, <https://doi.org/10.1038/s41598-023-43616-7>.
- [129] M.I. Hossain, M.A. Hasnat, Recent advancements in non-enzymatic electrochemical sensor development for the detection of organophosphorus pesticides in food and environment, *Heliyon* 9 (2023) e19299, <https://doi.org/10.1016/j.heliyon.2023.e19299>.
- [130] V.S. Manikandan, B. Adhikari, A. Chen, Nanomaterial based electrochemical sensors for the safety and quality control of food and beverages, *Analyst* 143 (2018) 4537–4554, <https://doi.org/10.1039/C8AN00497H>.
- [131] D. Capoferri, F. Della Pelle, M. Del Carlo, D. Compagnone, Affinity sensing strategies for the detection of pesticides in food, *Foods* 7 (2018), <https://doi.org/10.3390/foods7090148>.
- [132] A.G.-M. Ferrari, R.D. Crapnell, C.E. Banks, Electroanalytical overview: electrochemical sensing platforms for food and drink safety, *Biosensors* 11 (2021), <https://doi.org/10.3390/bios11080291>.
- [133] J. Kupai, M. Razali, S. Buyuktiyaki, R. Kecili, G. Szekely, Long-term stability and reusability of molecularly imprinted polymers, *Polym. Chem.* 8 (2017) 666–673, <https://doi.org/10.1039/C6PY01853J>.
- [134] M.R. Dunn, C.M. McCloskey, P. Buckley, K. Rhea, J.C. Chaput, Generating biologically stable TNA aptamers that function with high affinity and thermal stability, *J. Am. Chem. Soc.* 142 (2020) 7721–7724, <https://doi.org/10.1021/jacs.0c00641>.
- [135] Y. Le Basle, P. Chennell, N. Tokhadze, A. Astier, V. Sautou, Physicochemical stability of monoclonal antibodies: a review, *J. Pharmaceut. Sci.* 109 (2020) 169–190, <https://doi.org/10.1016/j.xphs.2019.08.009>.
- [136] S. Fiori, A. Scroccarello, F. Della Pelle, M. Del Carlo, D. Compagnone, Integrated paper/graphene 3D pop-up device for the quantitative sensing of carbaryl, *Sensor. Actuator. B Chem.* 399 (2024) 134768, <https://doi.org/10.1016/j.snb.2023.134768>.
- [137] K.F. Reardon, Practical monitoring technologies for cells and substrates in biomanufacturing, *Curr. Opin. Biotechnol.* 71 (2021) 225–230, <https://doi.org/10.1016/j.copbio.2021.08.006>.
- [138] G. Eisenbrand (Ed.), *Römp-Lexikon Lebensmittelchemie, second ed.*, Thieme, Stuttgart, 2006.

- [139] O.S. Ahmad, T.S. Bedwell, C. Esen, A. Garcia-Cruz, S.A. Piletsky, Molecularly imprinted polymers in electrochemical and optical sensors, *Trends Biotechnol.* 37 (2019) 294–309, <https://doi.org/10.1016/j.tibtech.2018.08.009>.
- [140] Y. Li, L. Luo, Y. Kong, Y. Li, Q. Wang, M. Wang, Y. Li, A. Davenport, B. Li, Recent advances in molecularly imprinted polymer-based electrochemical sensors, *Biosens. Bioelectron.* 249 (2024) 116018, <https://doi.org/10.1016/j.bios.2024.116018>.
- [141] R.D. Crapnell, N.C. Dempsey-Hibbert, M. Peeters, A. Tridente, C.E. Banks, Molecularly imprinted polymer based electrochemical biosensors: overcoming the challenges of detecting vital biomarkers and speeding up diagnosis, *Talanta Open* 2 (2020) 100018, <https://doi.org/10.1016/j.talo.2020.100018>.
- [142] Y. Saylan, S. Akgözüllü, H. Yavuz, S. Ünal, A. Denizli, Molecularly imprinted polymer based sensors for medical applications, *Sensors (Basel, Switzerland)* 19 (2019), <https://doi.org/10.3390/s19061279>.
- [143] X. Ni, X. Tang, D. Wang, J. Zhang, L. Zhao, J. Gao, H. He, P. Dramou, Research progress of sensors based on molecularly imprinted polymers in analytical and biomedical analysis, *J. Pharmaceut. Biomed. Anal.* 235 (2023) 115659, <https://doi.org/10.1016/j.jpba.2023.115659>.
- [144] E. Mazzotta, T. Di Giulio, C. Malatesta, Electrochemical sensing of macromolecules based on molecularly imprinted polymers: challenges, successful strategies, and opportunities, *Anal. Bioanal. Chem.* 414 (2022) 5165–5200, <https://doi.org/10.1007/s00216-022-03981-0>.
- [145] J.W. Lowdon, H. Diliën, P. Singla, M. Peeters, T.J. Cleij, B. van Grinsven, K. Eersels, MIPs for commercial application in low-cost sensors and assays - an overview of the current status quo, *Sensor. Actuator. B Chem.* 325 (2020) 128973, <https://doi.org/10.1016/j.snb.2020.128973>.
- [146] M. Caldara, J. Kulpa, J.W. Lowdon, T.J. Cleij, H. Diliën, K. Eersels, B. van Grinsven, Recent advances in molecularly imprinted polymers for glucose monitoring: from fundamental research to commercial application, *Chemosensors* 11 (2023) 32, <https://doi.org/10.3390/chemosensors11010032>.
- [147] D. Hernández-Ramírez, M. Franco-Guzmán, I.S. Ibarra-Ortega, G.A. Álvarez-Romero, L.E. Rebollo-Perales, Review—trends on the development of non-enzymatic electrochemical sensors modified with molecularly imprinted polymers for the quantification of glucose, *J. Electrochem. Soc.* 171 (2024) 77506, <https://doi.org/10.1149/1945-7111/ad5d1f>.
- [148] Y. Zhou, L. Li, J. Tong, X. Chen, W. Deng, Z. Chen, X. Xiao, Y. Yin, Q. Zhou, Y. Gao, X. Hu, Y. Wang, Advanced nanomaterials for electrochemical sensors: application in wearable tear glucose sensing technology, *J. Mater. Chem. B* 12 (2024) 6774–6804, <https://doi.org/10.1039/d4tb00790e>.
- [149] K. Murugesan, S. Das, K. Dutta, Molecularly imprinted polymers as bioreceptors in electrochemical biosensor (ECBS) for cholesterol detection, *Polymer-Plastics Technology and Materials* 62 (2023) 1477–1497, <https://doi.org/10.1080/25740881.2023.2221334>.
- [150] S.J. Cho, H.-B. Noh, M.-S. Won, C.-H. Cho, K.B. Kim, Y.-B. Shim, A selective glucose sensor based on direct oxidation on a bimetal catalyst with a molecular imprinted polymer, *Biosens. Bioelectron.* 99 (2018) 471–478, <https://doi.org/10.1016/j.bios.2017.08.022>.
- [151] T. Chen, S. Wei, Z. Cheng, J. Liu, Specific detection of monosaccharide by dual-channel sensing platform based on dual catalytic system constructed by bio-enzyme and bionic enzyme using molecular imprinting polymers, *Sensor. Actuator. B Chem.* 320 (2020) 128430, <https://doi.org/10.1016/j.snb.2020.128430>.
- [152] Z. Chen, C. Wright, O. Dincel, T.-Y. Chi, J. Kameoka, A low-cost paper glucose sensor with molecularly imprinted polyaniline electrode, *Sensors (Basel, Switzerland)* 20 (2020), <https://doi.org/10.3390/s20041098>.
- [153] A. Garcia-Cruz, O.S. Ahmad, A. Alanazi, E. Piletska, S.A. Piletsky, Generic sensor platform based on electro-responsive molecularly imprinted polymer nanoparticles (e-NanoMIPs), *Microsystems & nanoengineering* 6 (2020) 83, <https://doi.org/10.1038/s41378-020-00193-3>.
- [154] M. Caldara, J.W. Lowdon, G. van Wissen, A.G.-M. Ferrari, R.D. Crapnell, T. J. Cleij, H. Diliën, C.E. Banks, K. Eersels, B. van Grinsven, Dipstick sensor based on molecularly imprinted polymer-coated screen-printed electrodes for the single-shot detection of glucose in urine samples—from fundamental study toward point-of-care application, *Adv. Mater. Interfac.* 10 (2023), <https://doi.org/10.1002/admi.202300182>.
- [155] A. Okhokhonin, V. Stepanova, N. Malysheva, A. Matern, A. Kozytsina, Enzymeless electrochemical glucose sensor based on carboxylated multiwalled carbon nanotubes decorated with nickel (II) electrocatalyst and self-assembled molecularly imprinted polyethylenimine, *Electroanalysis* 33 (2021) 111–119, <https://doi.org/10.1002/elan.202060177>.
- [156] A. Goyal, T. Sakata, Development of a redox-label-doped molecularly imprinted polymer on β -cyclodextrin/reduced graphene oxide for electrochemical detection of a stress biomarker, *ACS Omega* 7 (2022) 33491–33499, <https://doi.org/10.1021/acsomega.2c04423>.
- [157] E. Kellens, H. Bové, T. Vandenryt, J. Lambrechts, J. Dekens, S. Drijkoningen, J. D'Haen, W. de Ceuninck, R. Thoelen, T. Junkers, K. Haenen, A. Ethirajan, Micro-patterned molecularly imprinted polymer structures on functionalized diamond-coated substrates for testosterone detection, *Biosens. Bioelectron.* 118 (2018) 58–65, <https://doi.org/10.1016/j.bios.2018.07.032>.
- [158] M.H. Mahnashi, A.M. Mahmoud, K. Alhazzani, A. Az, M.M. Algahtani, A. M. Alaseem, Y.S. Alqahtani, M.M. El-Wakil, Enhanced molecular imprinted electrochemical sensing of histamine based on signal reporting nanohybrid, *Microchem. J.* 168 (2021) 106439, <https://doi.org/10.1016/j.microc.2021.106439>.
- [159] I. Alam, B. Lertanantawong, T. Sutthibutpong, P. Punnakitkashem, P. Asanithi, Molecularly imprinted polymer-amyloid fibril-based electrochemical biosensor for ultrasensitive detection of tryptophan, *Biosensors* 12 (2022), <https://doi.org/10.3390/bios12050291>.
- [160] Y. Li, L. Luo, M. Nie, A. Davenport, Y. Li, B. Li, K.-L. Choy, A graphene nanoplatelet-polydopamine molecularly imprinted biosensor for Ultratrace creatinine detection, *Biosens. Bioelectron.* 216 (2022) 114638, <https://doi.org/10.1016/j.bios.2022.114638>.
- [161] S.S.M. Hassan, A.H. Kamel, M.A. Fathy, All-solid-state paper-based potentiometric combined sensor modified with reduced graphene oxide (rGO) and molecularly imprinted polymer for monitoring losartan drug in pharmaceuticals and biological samples, *Talanta* 253 (2023) 123907, <https://doi.org/10.1016/j.talanta.2022.123907>.
- [162] M.H. Mahnashi, A.M. Mahmoud, K. Alhazzani, A.Z. Alanazi, A.M. Alaseem, M. M. Algahtani, M.M. El-Wakil, Ultrasensitive and selective molecularly imprinted electrochemical oxaliplatin sensor based on a novel nitrogen-doped carbon nanotubes/Ag@Cu MOF as a signal enhancer and reporter nanohybrid, *Microchim. Acta* 188 (2021) 124, <https://doi.org/10.1007/s00604-021-04781-6>.
- [163] B. Bozal-Palabiyik, M. Lettieri, B. Uslu, G. Marrazza, Electrochemical detection of vascular endothelial growth factor by molecularly imprinted polymer, *Electroanalysis* 31 (2019) 1458–1464, <https://doi.org/10.1002/elan.201900185>.
- [164] S.M. Cerqueira, R. Fernandes, F.T. Moreira, M.G.F. Sales, Development of an electrochemical biosensor for Galectin-3 detection in point-of-care, *Microchem. J.* 164 (2021) 105992, <https://doi.org/10.1016/j.microc.2021.105992>.
- [165] M.d.L. Gonçalves, L.A.N. Truta, M.G.F. Sales, F.T.C. Moreira, Electrochemical point-of care (PoC) determination of interleukin-6 (IL-6) using a pyrrole (py) molecularly imprinted polymer (MIP) on a carbon-screen printed electrode (C-spe), *Anal. Lett.* 54 (2021) 2611–2623, <https://doi.org/10.1080/00032719.2021.1879108>.
- [166] S. Campuzano, M. Pedrero, P. Yáñez-Sedeño, J.M. Pingarrón, Antifouling (Bio) materials for electrochemical (Bio)sensing, *Int. J. Mol. Sci.* 20 (2019), <https://doi.org/10.3390/ijms20020423>.
- [167] P.-H. Lin, B.-R. Li, Antifouling strategies in advanced electrochemical sensors and biosensors, *Analyst* 145 (2020) 1110–1120, <https://doi.org/10.1039/c9an02017a>.
- [168] S. Saxena, P. Sen, L. Soleymani, T. Hoare, Anti-fouling polymer or peptide-modified electrochemical biosensors for improved biosensing in complex media, *Advanced Sensor Research* 3 (2024), <https://doi.org/10.1002/adsr.202300170>.
- [169] G. Song, H. Han, Z. Ma, Anti-fouling strategies of electrochemical sensors for tumor markers, *Sensors (Basel, Switzerland)* 23 (2023), <https://doi.org/10.3390/s23115202>.
- [170] L. Zhou, X. Li, B. Zhu, B. Su, An overview of antifouling strategies for electrochemical analysis, *Electroanalysis* 34 (2022) 966–975, <https://doi.org/10.1002/elan.202100406>.
- [171] M.J. Russo, M. Han, P.E. Desroches, C.S. Manasa, J. Dennaoui, A.F. Quigley, R.M. I. Kapsa, S.E. Moulton, R.M. Gujt, G.W. Greene, S.M. Silva, Antifouling strategies for electrochemical biosensing: mechanisms and performance toward point of care based diagnostic applications, *ACS Sens.* 6 (2021) 1482–1507, <https://doi.org/10.1021/acssensors.1c00390>.
- [172] Y. Choi, H.-V. Tran, T.R. Lee, Self-assembled monolayer coatings on gold and silica surfaces for antifouling applications: a review, *Coatings* 12 (2022) 1462, <https://doi.org/10.3390/coatings12101462>.
- [173] C. Moonla, M. Reynoso, A. Casanova, A.-Y. Chang, O. Djassemi, A. Balaje, A. Abbas, Z. Li, K. Mahato, J. Wang, Continuous ketone monitoring via wearable microneedle patch platform, *ACS Sens.* 9 (2024) 1004–1013, <https://doi.org/10.1021/acssensors.3c02677>.
- [174] D.-S. Shin, Z. Matharu, J. You, C. Siltanen, T. Vu, V.K. Raghunathan, G. Stybayeva, A.E. Hill, A. Revzin, Sensing conductive hydrogels for rapid detection of cytokines in blood, *Adv. Healthcare Mater.* 5 (2016) 659–664, <https://doi.org/10.1002/adhm.201500571>.
- [175] X. Zhu, Y. Zhai, X. Qin, Y. Ding, Y. Wang, An antifouling coating that enables electrochemical biosensing of MeCa gene in complex samples, *Chem. Eng. J.* 483 (2024) 148975, <https://doi.org/10.1016/j.cej.2024.148975>.
- [176] Z. Xi, K. Wei, Q. Wang, M.J. Kim, S. Sun, Y. Fung, X. Xia, Nickel-platinum nanoparticles as peroxidase mimics with a record high catalytic efficiency, *J. Am. Chem. Soc.* 143 (2021) 2660–2664, <https://doi.org/10.1021/jacs.0c12605>.
- [177] M. Adeel, M.M. Rahman, I. Caligiuri, V. Canzonieri, F. Rizzolio, S. Daniele, Recent advances of electrochemical and optical enzyme-free glucose sensors operating at physiological conditions, *Biosens. Bioelectron.* 165 (2020) 112331, <https://doi.org/10.1016/j.bios.2020.112331>.
- [178] K. Shim, W.-C. Lee, M.-S. Park, M. Shahabuddin, Y. Yamauchi, M.S.A. Hossain, Y.-B. Shim, J.H. Kim, Au decorated core-shell structured Au@Pt for the glucose oxidation reaction, *Sensor. Actuator. B Chem.* 278 (2019) 88–96, <https://doi.org/10.1016/j.snb.2018.09.048>.
- [179] J. Zhu, S. Liu, Z. Hu, X. Zhang, N. Yi, K. Tang, M.G. Dexeimer, X. Lian, Q. Wang, J. Yang, J. Gray, H. Cheng, Laser-induced graphene non-enzymatic glucose sensors for on-body measurements, *Biosens. Bioelectron.* 193 (2021) 113606, <https://doi.org/10.1016/j.bios.2021.113606>.
- [180] X. Strakosas, J. Selberg, P. Pansodtee, N. Yonas, P. Manapongpun, M. Teodorescu, M. Rolandi, A non-enzymatic glucose sensor enabled by bioelectronic pH control, *Sci. Rep.* 9 (2019) 10844, <https://doi.org/10.1038/s41598-019-46302-9>.
- [181] X. Zhu, Y. Ju, J. Chen, D. Liu, H. Liu, Nonenzymatic wearable sensor for electrochemical analysis of perspiration glucose, *ACS Sens.* 3 (2018) 1135–1141, <https://doi.org/10.1021/acssensors.8b00168>.
- [182] Y. Dang, X. Guan, Y. Zhou, C. Hao, Y. Zhang, S. Chen, Y. Ma, Y. Bai, Y. Gong, Y. Gao, Biocompatible PB/Ti3C2 hybrid nanocomposites for the non-enzymatic electrochemical detection of H2O2 released from living cells, *Sensor. Actuator. B Chem.* 319 (2020) 128259, <https://doi.org/10.1016/j.snb.2020.128259>.

- [183] T. Mosmann, Rapid colorimetric assay for cellular growth and survival: application to proliferation and cytotoxicity assays, *J. Immunol. Methods* 65 (1983) 55–63, [https://doi.org/10.1016/0022-1759\(83\)90303-4](https://doi.org/10.1016/0022-1759(83)90303-4).
- [184] Y. Chen, Y. Sun, Y. Li, Z. Wen, X. Peng, Y. He, Y. Hou, J. Fan, G. Zang, Y. Zhang, A wearable non-enzymatic sensor for continuous monitoring of glucose in human sweat, *Talanta* 278 (2024) 126499, <https://doi.org/10.1016/j.talanta.2024.126499>.
- [185] R. Fan, T.L. Andrew, Perspective—challenges in developing wearable electrochemical sensors for longitudinal health monitoring, *J. Electrochem. Soc.* 167 (2020) 37542, <https://doi.org/10.1149/1945-7111/ab67b0>.
- [186] Z. Li, Y. Wang, A. Kozbial, G. Shenoy, F. Zhou, R. McGinley, P. Ireland, B. Morganstein, A. Kunkel, S.P. Surwade, L. Li, H. Liu, Effect of airborne contaminants on the wettability of supported graphene and graphite, *Nat. Mater.* 12 (2013) 925–931, <https://doi.org/10.1038/NMAT3709>.
- [187] A. Behrent, V. Borggraefe, A.J. Baeumner, Laser-induced graphene trending in biosensors: understanding electrode shelf-life of this highly porous material, *Anal. Bioanal. Chem.* 416 (2024) 2097–2106, <https://doi.org/10.1007/s00216-023-05082-y>.
- [188] L. Zhang, L. Wang, J. Li, C. Cui, Z. Zhou, L. Wen, Surface engineering of laser-induced graphene enables long-term monitoring of on-body uric acid and pH simultaneously, *Nano Lett.* 22 (2022) 5451–5458, <https://doi.org/10.1021/acs.nanolett.2c01500>.
- [189] J.J. Beck, V. Alenicheva, K.L. Rahn, M.J. Russo, T.A. Baldo, C.S. Henry, Evaluating the performance of an inexpensive, commercially available, NFC-powered and smartphone controlled potentiostat for electrochemical sensing, *Electroanalysis* 35 (2023), <https://doi.org/10.1002/elan.202200552>.
- [190] L. Gonzalez-Macia, Y. Li, K. Zhang, E. Nunez-Bajo, G. Barandun, Y. Cotur, T. Asfour, S. Olenik, P. Coatsworth, J. Herrington, F. Güder, NFC-enabled potentiostat and nitrocellulose-based metal electrodes for electrochemical lateral flow assay, *Biosens. Bioelectron.* 251 (2024) 116124, <https://doi.org/10.1016/j.bios.2024.116124>.
- [191] K. Krarakai, S. Klangphukhiew, S. Kulchat, R. Patramanon, Smartphone-based NFC potentiostat for wireless electrochemical sensing, *Appl. Sci.* 11 (2021) 392, <https://doi.org/10.3390/app11010392>.
- [192] P. Lathiya, J. Wang, Near-field communications (NFC) for wireless power transfer (WPT): an overview, in: M. Zelligui (Ed.), *Wireless Power Transfer – Recent Development, Applications and New Perspectives*, IntechOpen, 2021.
- [193] Y. Gu, C.-C. Chen, Eliminating the interference of oxygen for sensing hydrogen peroxide with the polyaniline modified electrode, *Sensors (Basel, Switzerland)* 8 (2008) 8237–8247, <https://doi.org/10.3390/s8128237>.
- [194] M. Etienne, T.X.H. Le, T. Nasir, G. Herzog, Electrochemical filter to remove oxygen interference locally, rapidly, and temporarily for sensing applications, *Anal. Chem.* 92 (2020) 7425–7429, <https://doi.org/10.1021/acs.analchem.0c00395>.